Fast timing per la nuova frontiera della Positron Emission Tomography

Marco Pizzichemi
Università degli Studi di Milano Bicocca

Outline

- ➔ Positron Emission Tomography
  - ➢ Introduction to PET
  - ➢ Main research trends
  - ➢ Time of Flight PET

- ➔ Research in PET @ UniMib
  - ➢ Some history: ClearPEM and EndoTOFPET
  - ➢ Current research activities

Introduction

Positron Emission Tomography

In vivo imaging technique to quantitatively measure the 3D distribution of radiolabeled molecules

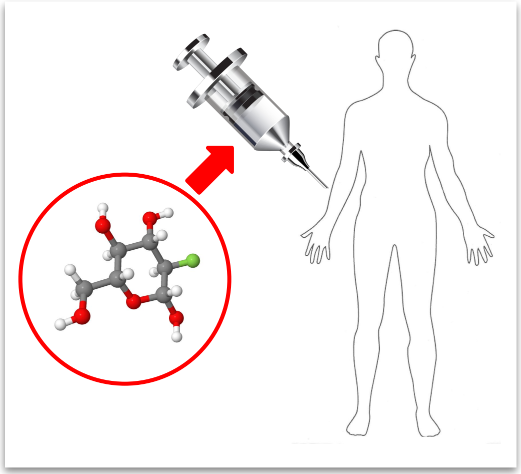

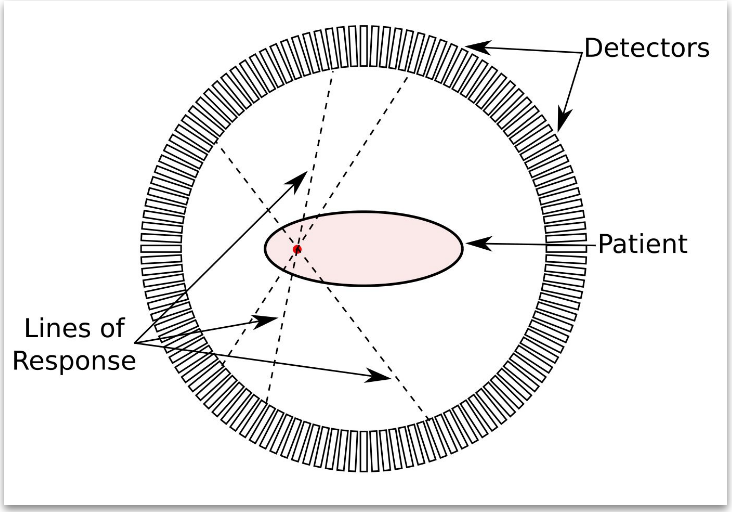

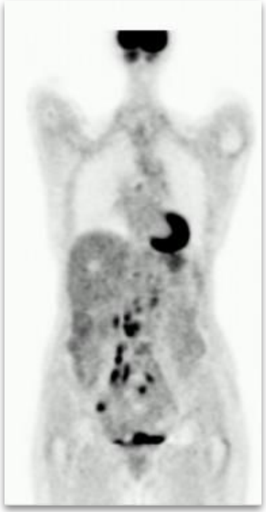

Molecule labeled with **beta+** emitter, detection of gamma rays emitted by positron **annihilation**

Positron Emission Tomography

In vivo imaging technique to quantitatively measure the 3D distribution of radiolabeled molecules

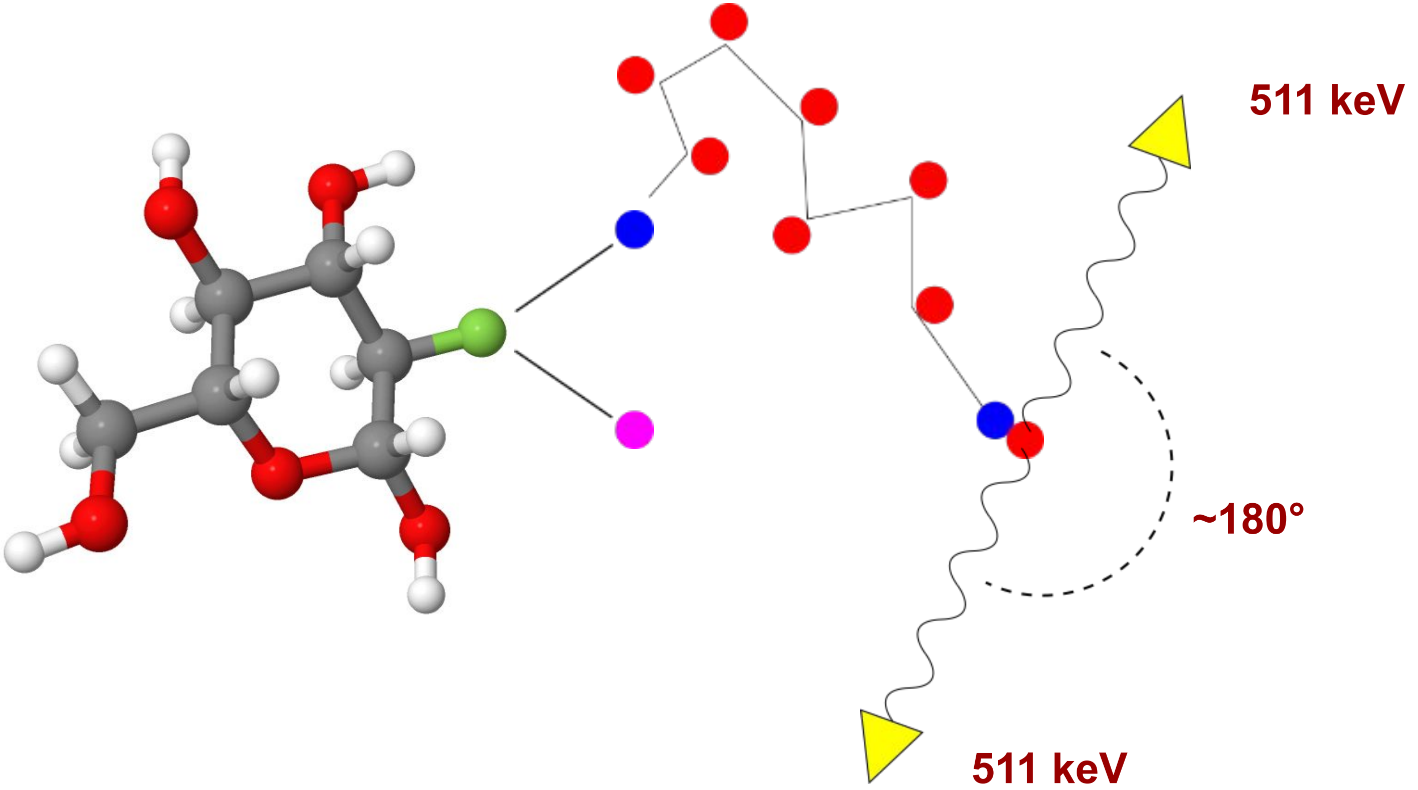

PET and medical imaging modalities

TABLE I. – *A list of the most common Imaging techniques with their main performance related to molecular imaging.*

Imaging technique	Source of signal	Spatial resolution	Sensitivity (mol/l)	Quantitative/Morphological information
PET	γ-rays (511 keV)	1–4 mm	10^{-11}–10^{-12}	+++/+
SPECT	γ-rays (< 300 keV)	0.3–10 mm	10^{-10}–10^{-11}	++/+
Optical bioluminescence	Visible light	3–5 mm	10^{-15}–10^{-17} (theoretical)	+(++)/n.a.
Optical fluorescence	Visible light and NIR	2–3 mm	10^{-9}–10^{-12} (probable)	+(++)/n.a.
MRI	Radio waves	25–100 μm	10^{-3}–10^{-5}	++/+++
CT	X-rays (40–120 keV)	10–200 μm	n.a	n.a./+++

PET applications:

- ➔ Oncology
- ➔ Neurology
- ➔ Cardiology
- ➔ Drug development
- ➔ More...

The PET system

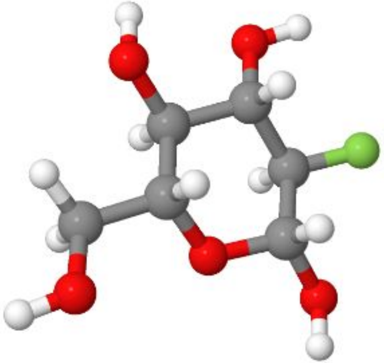

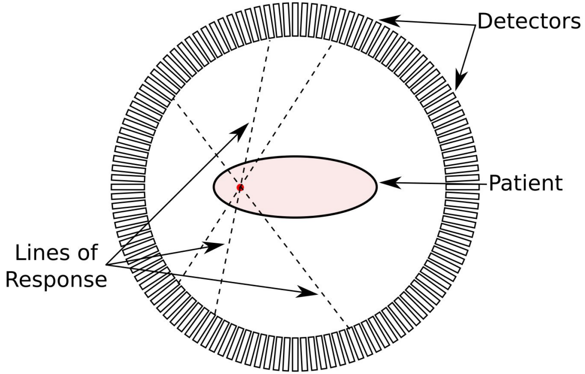

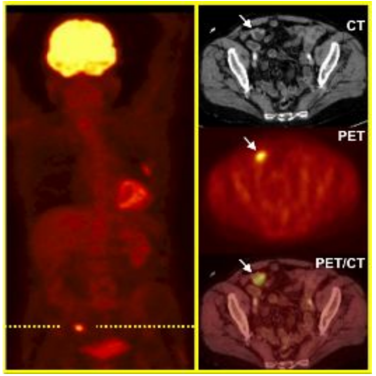

Biology

Detector

Software

Detection of radiation in PET

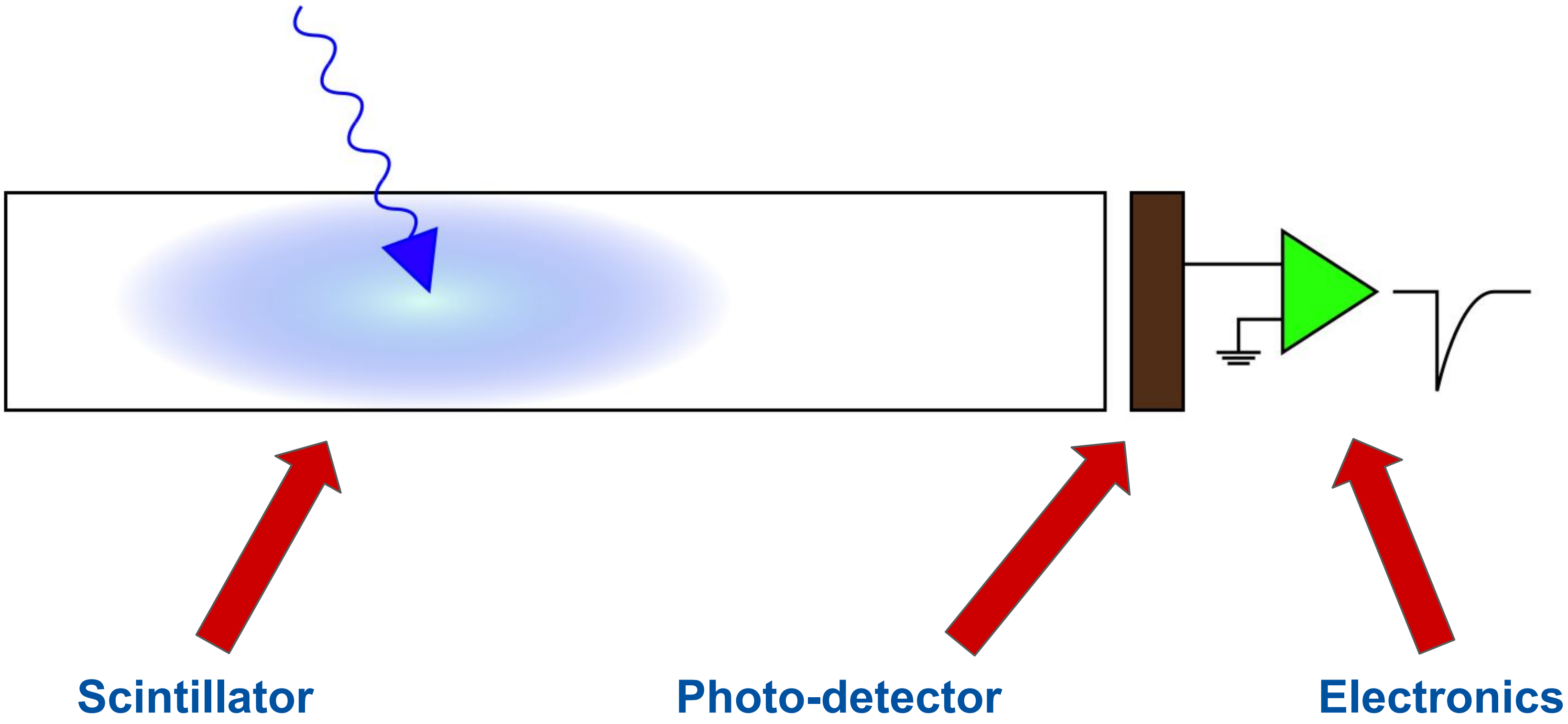

PET geometry

➔ Cylindrical coverage and thick, dense scintillators to maximize **sensitivity**

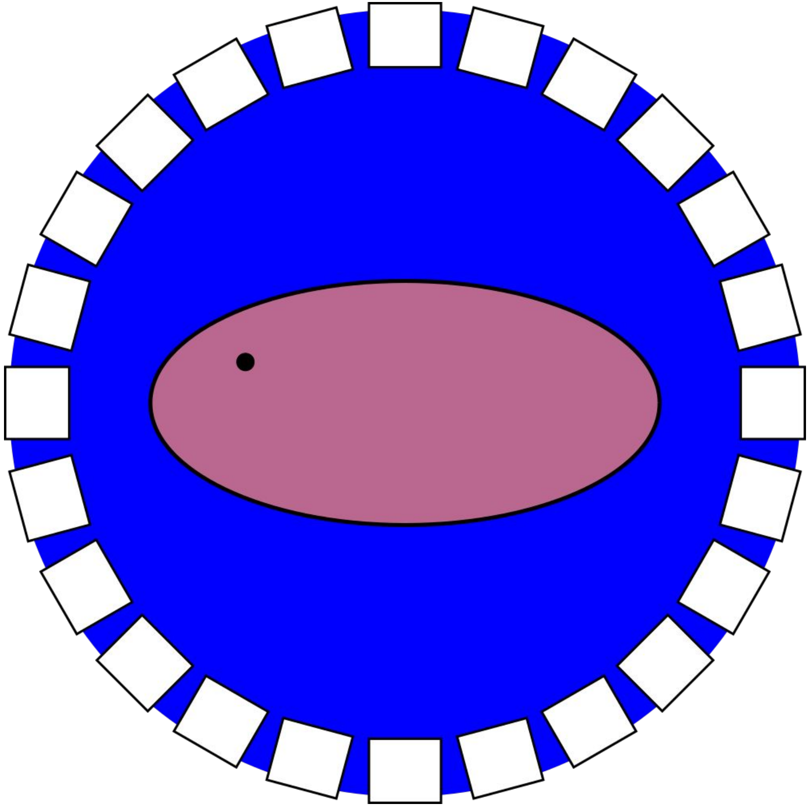

PET geometry

➔ Cylindrical coverage and thick, dense scintillators to maximize **sensitivity**

➔ **Spatial resolution** defined by crystal (or detector) section

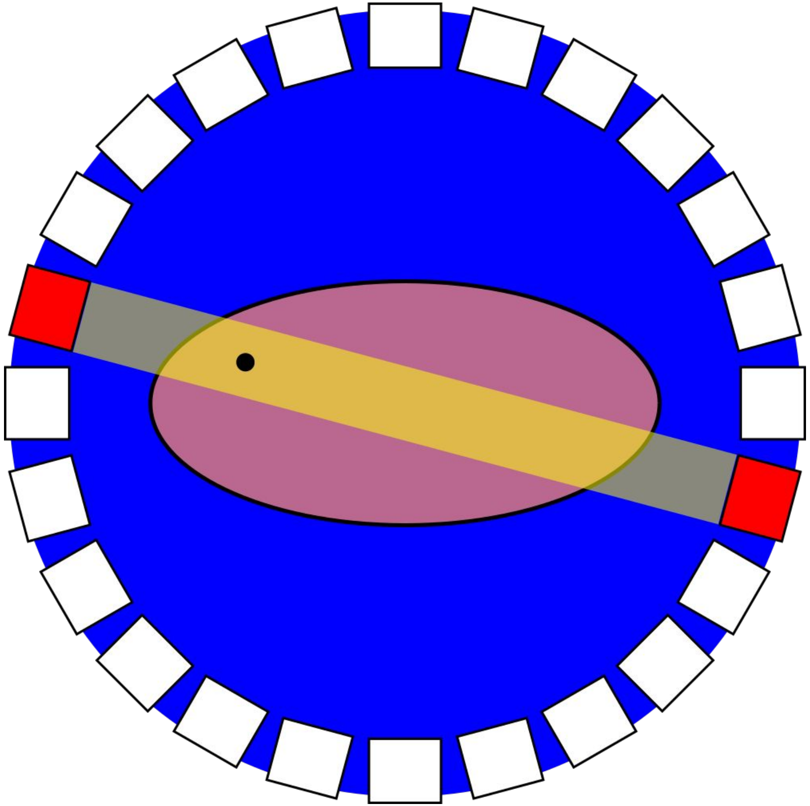

PET geometry

- ➔ Cylindrical coverage and thick, dense scintillators to maximize **sensitivity**
- ➔ **Spatial resolution** defined by crystal (or detector) section
- ➔ Segmentation improves spatial resolution..

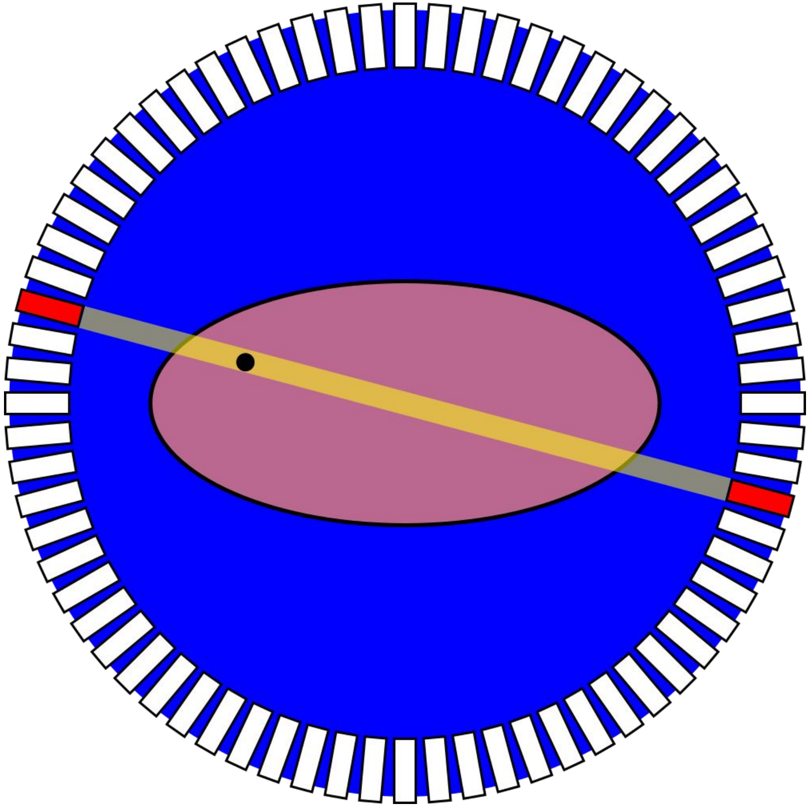

PET geometry

UNIVERSITA' DEGLI STUDI DI MILANO BICOCCA

- ➔ Cylindrical coverage and thick, dense scintillators to maximize **sensitivity**
- ➔ **Spatial resolution** defined by crystal (or detector) section
- ➔ Segmentation improves spatial resolution..
- ➔ ...but at the same time resolution degrades due to parallax effect

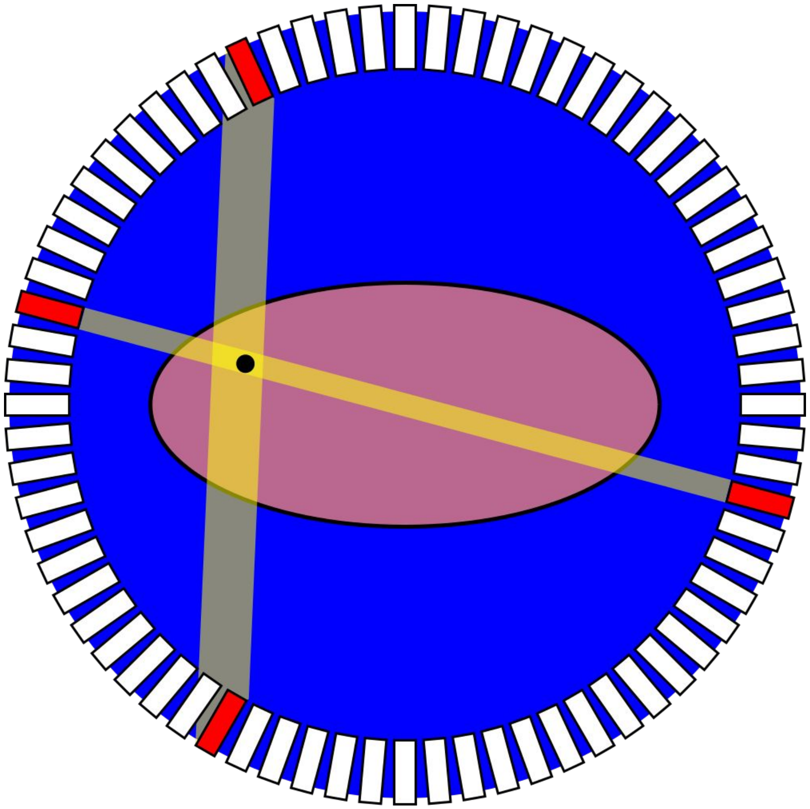

PET geometry

- ➔ Cylindrical coverage and thick, dense scintillators to maximize **sensitivity**
- ➔ **Spatial resolution** defined by crystal (or detector) section
- ➔ Segmentation improves spatial resolution..
- ➔ ...but at the same time resolution degrades due to parallax effect
- ➔ This can be recovered if the **Depth of Interaction** (DOI) of the gamma ray is measured

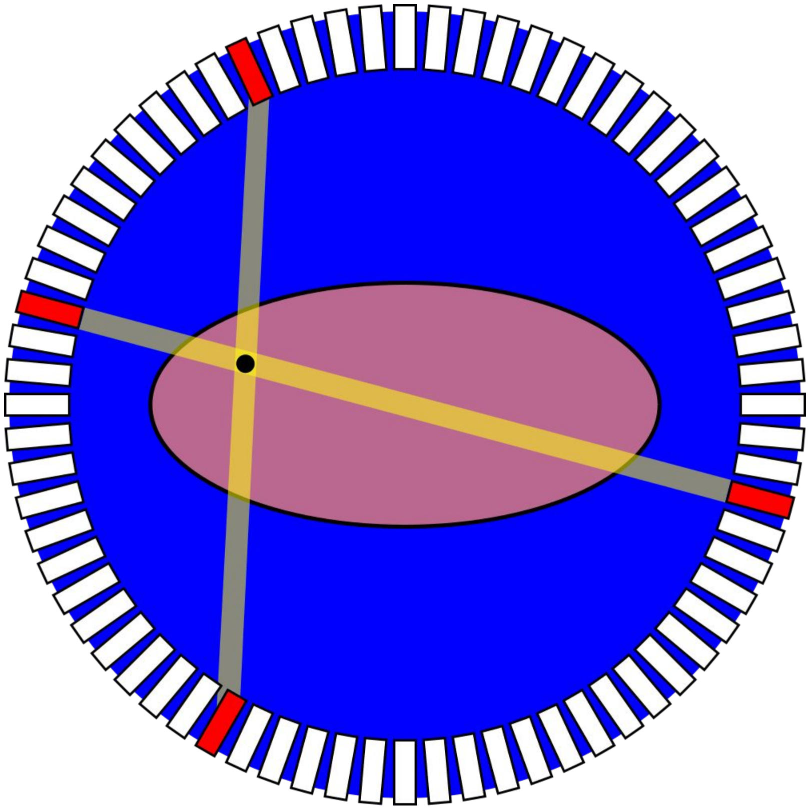

Impact of DOI on image quality

^{22}Na source moved on a grid of 5 mm pitch

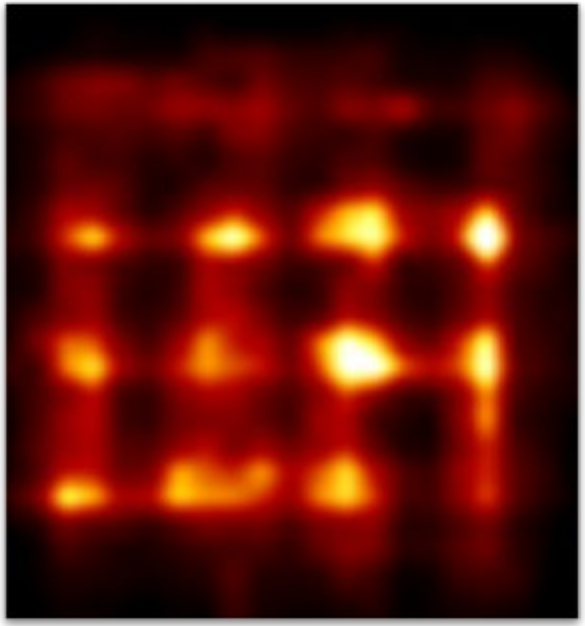

Without DOI

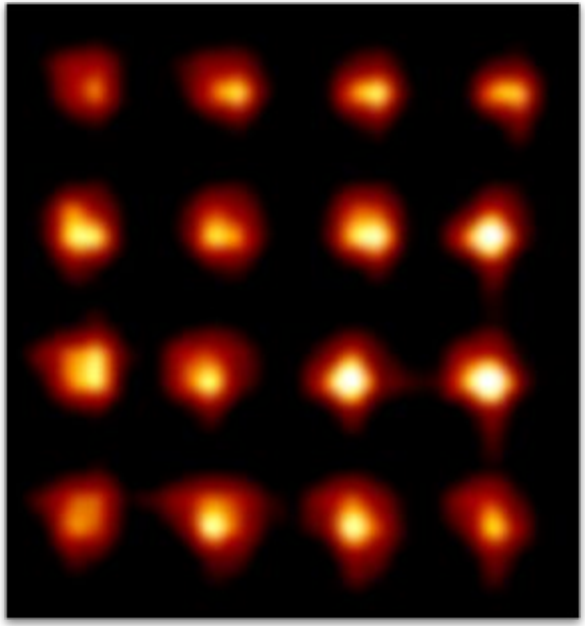

With DOI

PET events

➔ A **true coincidence** is identified if two detected gammas have:

- ➢ Energy in the 511 keV energy window
- ➢ Difference in time of arrival within the coincidence window

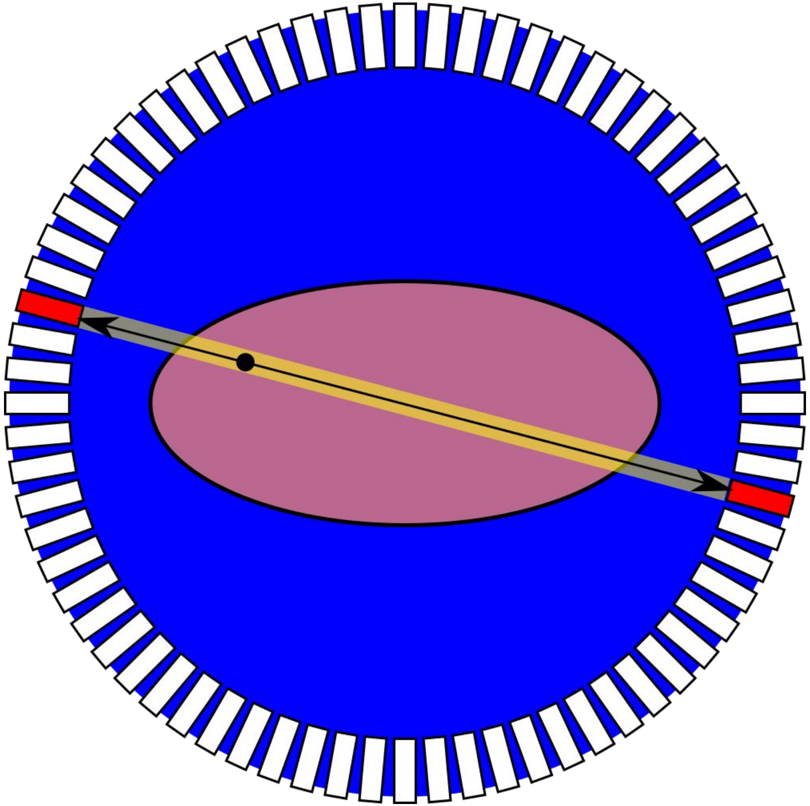

PET events

- ➔ A **true coincidence** is identified if two detected gammas have:
  - ➢ Energy in the 511 keV energy window
  - ➢ Difference in time of arrival within the coincidence window

- ➔ The gammas can undergo **scatter** in the patient body, changing direction and resulting in wrong LOR reconstruction:
  - ➢ Good **energy resolution** is needed to reject these events (typically 10% FWHM)

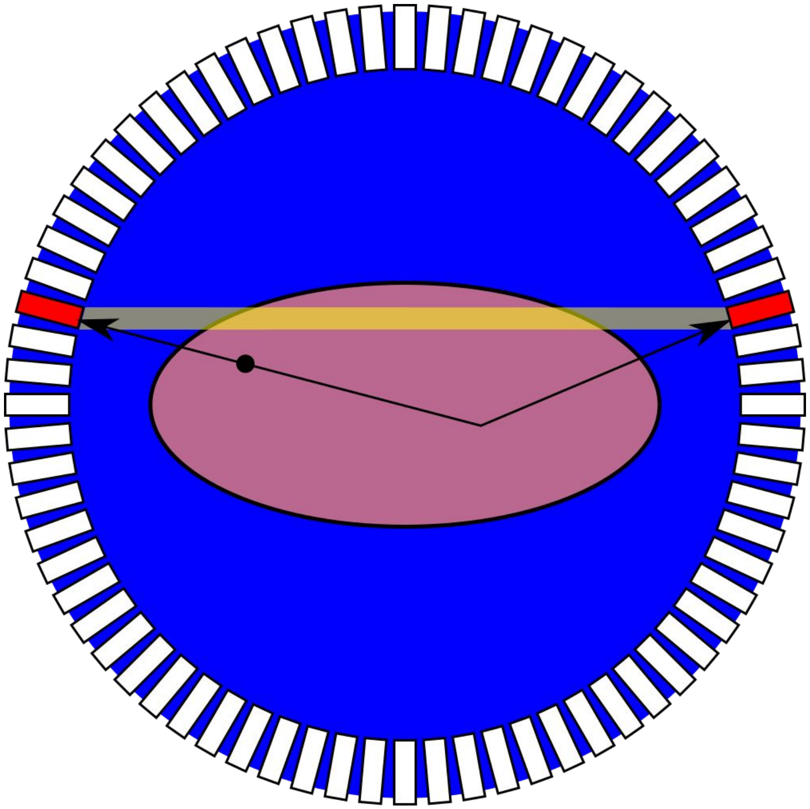

PET events

➔ A **true coincidence** is identified if two detected gammas have:

- ➢ Energy in the 511 keV energy window
- ➢ Difference in time of arrival within the coincidence window

➔ The gammas can undergo **scatter** in the patient body, changing direction and resulting in wrong LOR reconstruction:

- ➢ Good **energy resolution** is needed to reject these events (typically 10% FWHM)

➔ The coincidence can be assigned to two gammas coming from different annihilation events that fall **randomly** within the coincidence window:

- ➢ Good **timing resolution** is needed to minimize the probability of these false coincidences (depends on the scanner diameter)

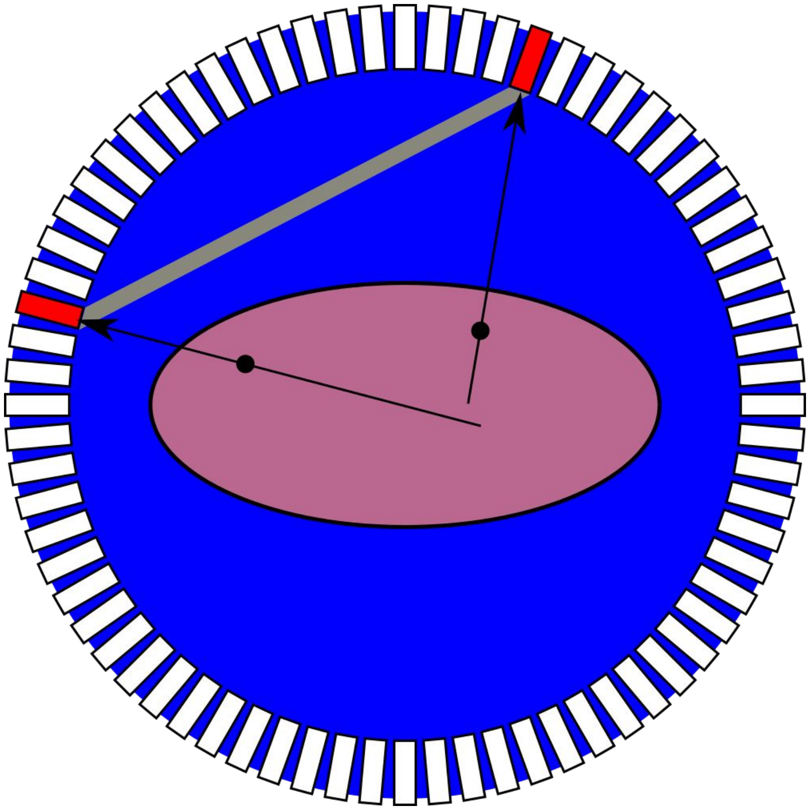

Main research trends in PET detectors

- Improve system sensitivity
  - Time-of-Flight PET
  - Organ dedicated scanners
  - Total body scanner

- Develop multimodality
  - Integration with MR
  - Integration with US

Time of Flight (TOF) PET

Compute the difference in time of arrival of gammas:

➔ Improve event localization along LORs

$$\Delta x = c\frac{\Delta t}{2}$$

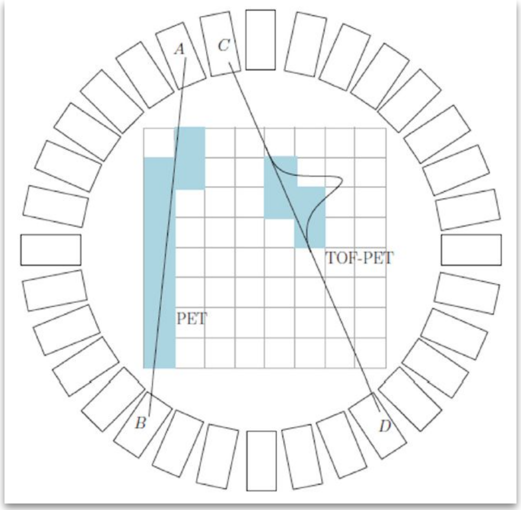

S. Surti, J.S. Karp - Physica Medica 32 (2016) 12-22

Time of Flight (TOF) PET

Compute the difference in time of arrival of gammas:

➔ Improve event localization along LORs

$$\Delta x = c\frac{\Delta t}{2}$$

➔ Decrease noise correlation in overlapping LORs, improve signal-to-noise ratio (SNR)

$$SNR_{TOF} \sim \sqrt{\frac{D}{\Delta x}} \cdot SNR_{CONV}$$

D = effective object diameter

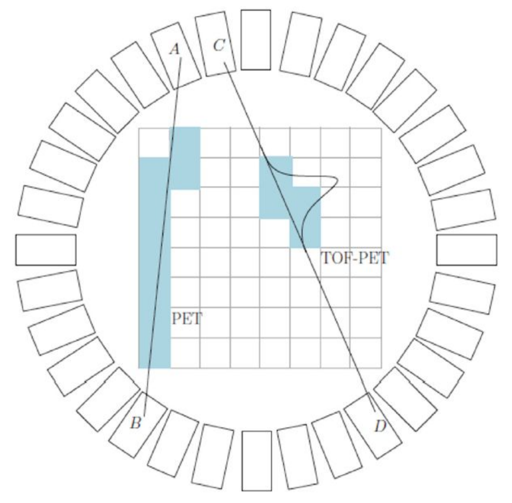

S. Surti, J.S. Karp - Physica Medica 32 (2016) 12-22

Time resolution (ns)	Δx (cm)	TOF NEC gain	TOF SNR gain
0.1	1.5	26.7	5.2
0.3	4.5	8.9	3.0
0.6	9.0	4.4	2.1
1.2	18.0	2.2	1.5
2.7	40.0	1.0	1.0

M. Conti - Eur J Nucl Med Mol Imaging (2011) 38: 1147-1157

Benefits of TOF

➔ Improved **lesion detectability** while keeping scanning time constant

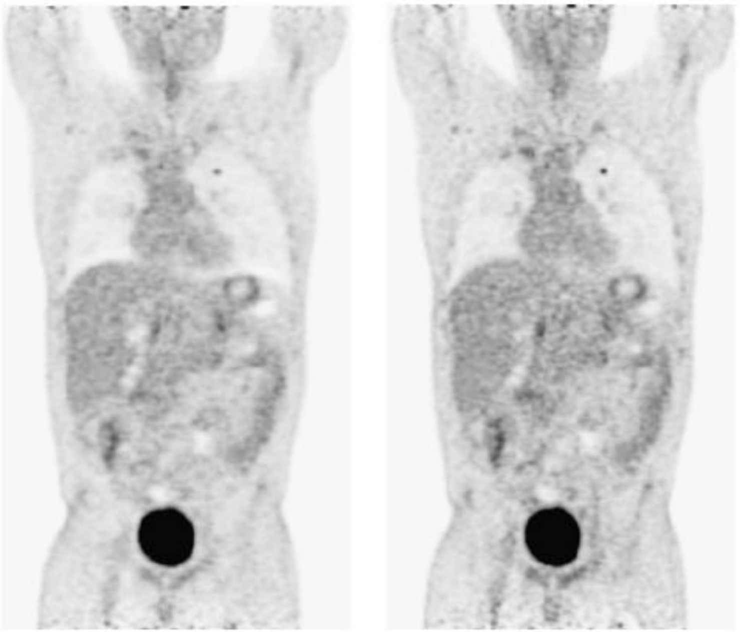

Fig. 1 Coronal images reconstructed from a non-TOF scan (*left*) and a TOF scan (*right*) in a patient with lung cancer. The acquisition time was 3 min per bed position for both images. At the same number of counts, the image quality is better with the TOF reconstruction

M. Conti - Eur J Nucl Med Mol Imaging (2011) 38: 1147-1157

Benefits of TOF

➔ Improved **lesion detectability** while keeping scanning time constant

➔ Reduced **scan time** for the same lesion detectability

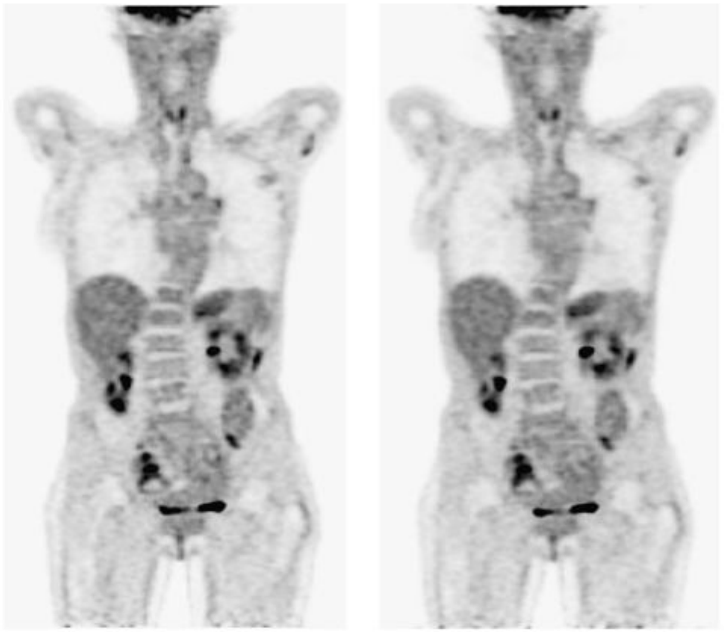

Fig. 2 Coronal images reconstructed from a non-TOF scan (*left*) and a TOF scan (*right*). The acquisition time was 2 min per bed position for the non-TOF scan and 1 min per bed position for the TOF scan. The quality of the non-TOF image and that of the TOF image with half of the counts are similar

M. Conti - Eur J Nucl Med Mol Imaging (2011) 38: 1147-1157

Benefits of TOF

- ➔ Improved **lesion detectability** while keeping scanning time constant
- ➔ Reduced **scan time** for the same lesion detectability
- ➔ **Fewer iteration** of reconstruction algorithms required to maximize lesion contrast -> lower image noise

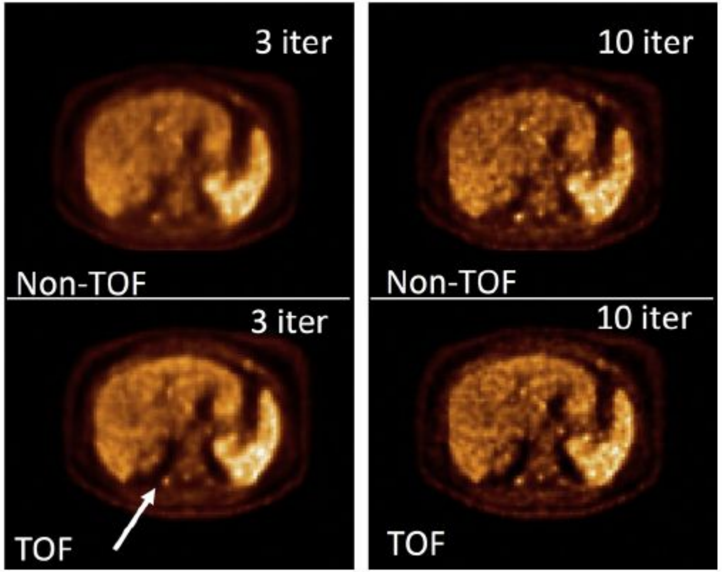

Figure 2. Reconstructed transverse slices of a clinical ^{18}F-FDG study. As indicated, images are shown for Non-TOF and TOF reconstruction and for iterations 3 and 10 of the reconstruction algorithm. The arrow indicates the lesion for which an accurate SUV is measured after 3 iterations of the TOF reconstruction algorithm.

S. Surti, J.S. Karp - Physica Medica 32 (2016) 12-22

Benefits of TOF

- ➔ Improved **lesion detectability** while keeping scanning time constant
- ➔ Reduced **scan time** for the same lesion detectability
- ➔ **Fewer iteration** of reconstruction algorithms required to maximize lesion contrast -> lower image noise
- ➔ Better lesion detectability for **larger objects**

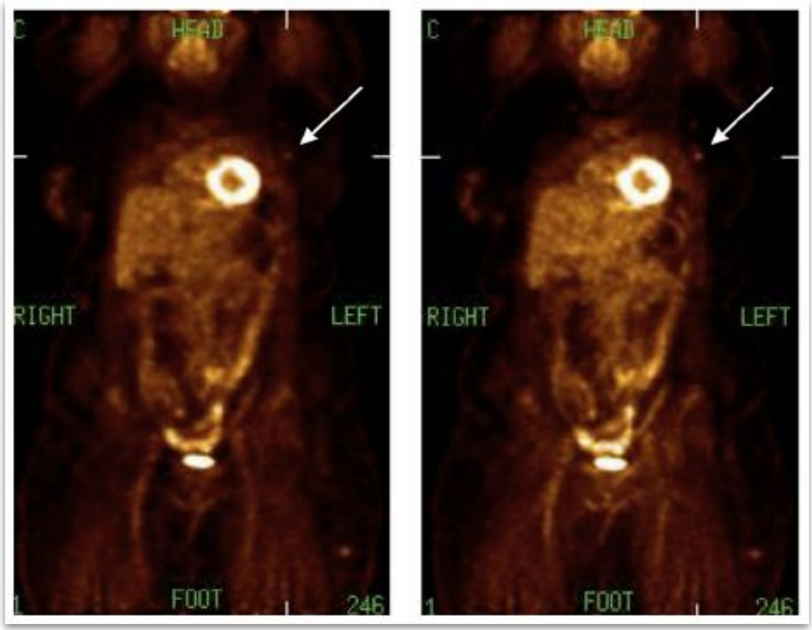

S. Surti, J.S. Karp - Physica Medica 32 (2016) 12-22

Benefits of TOF

- ➔ Improved **lesion detectability** while keeping scanning time constant
- ➔ Reduced **scan time** for the same lesion detectability
- ➔ **Fewer iteration** of reconstruction algorithms required to maximize lesion contrast -> lower image noise
- ➔ Better lesion detectability for **larger objects**
- ➔ Better image reconstruction for **limited angle** PET acquisitions

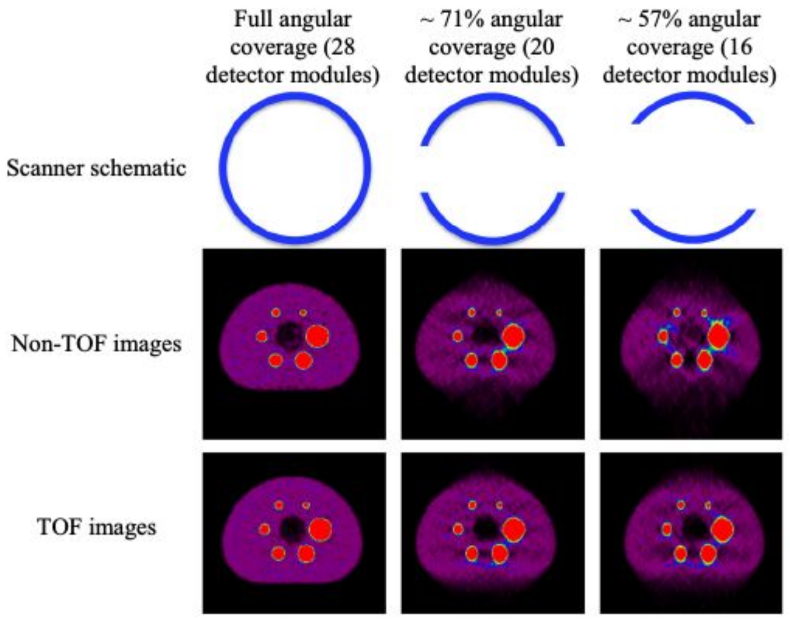

Figure 4. Reconstructed images from a NEMA image quality phantom using full or partial angular data acquired on a clinical TOF PET/CT. The six hot spheres in a ring have diameters of 37, 28, 22, 17, 13, and 10 mm and have an activity uptake of 9.7:1 with respect to background. The central cold region is a lung insert.

S. Surti, J.S. Karp - Physica Medica 32 (2016) 12-22

PET @ Bicocca: some history...

ClearPEM-Sonic (2010-2017)

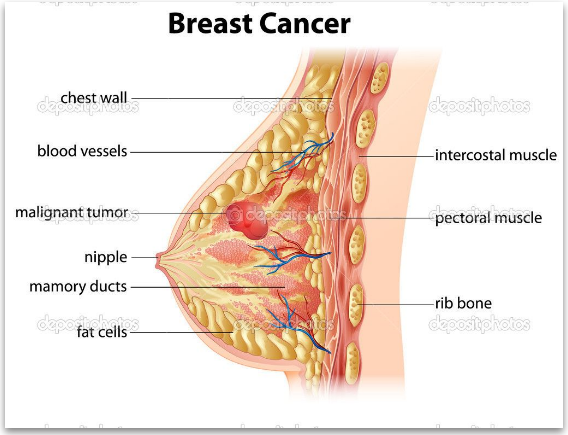

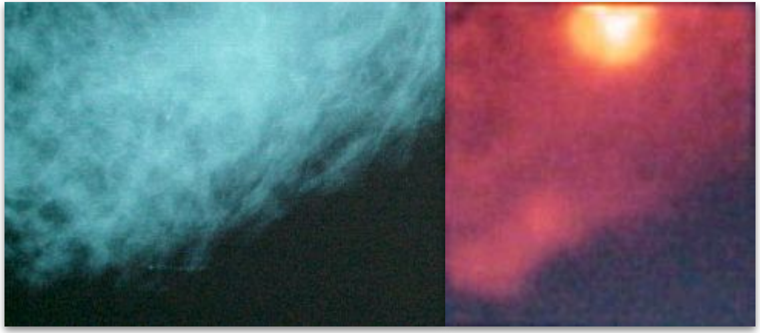

X-Ray PEM

- ➔ **Target:** breast cancer
  - ➢ 1 over 8 women affected during lifetime, 2nd cancer-related cause of death in women
  - ➢ Survival rate dramatically improves if diagnosed in early stage
- ➔ **Issues:** standard detection techniques (X-rays) suffer from low specificity
- ➔ **Goal:** improve sensitivity and spatial resolution (for breast)
  - ➢ Better specific sensitivity for breast
  - ➢ Very high spatial resolution

ClearPEM-Sonic (2010-2017)

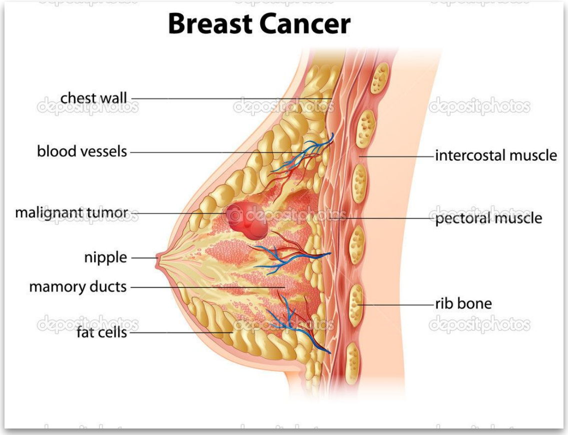

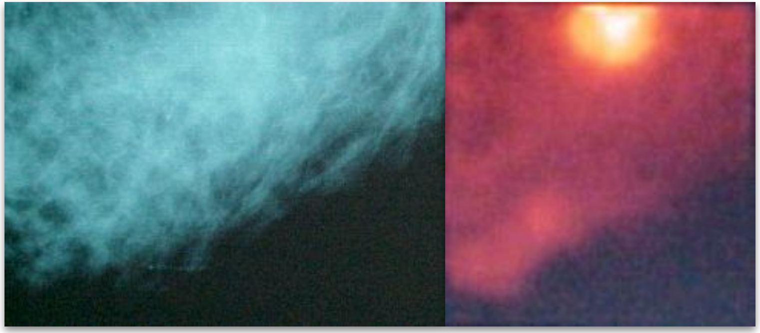

➔ International collaboration led by the **Crystal Clear Collaboration** at CERN:

The European Organisation for Nuclear Research (CERN), Geneva, Switzerland
The Vrije Universiteit Brussel (VUB), Brussels, Belgium
The Laboratório de Instrumentacão e Física Experimantal de Partículas (LIP), Lisbon, Portugal
The Université de la Mediterranée (Aix-Marseille II), Marseilles, France
Assistance-Publique-Hopitaux de Marseille (AP/HM), Marseilles, France
Deutsches Krebsforschungszentrum (DKFZ)
Institut Paoli – Calmettes (IPC), Marseilles, France
Laboratoire de Mécanique et d'Acoustique (LMA), CNRS, Marseilles, France
Università degli Studi di Milano-Bicocca (UNIMIB), Milano, Italy
The Universiteit Gent, Gent, Belgium
Supersonic Imagine, Aix-en-Provence, France
PETsys-Medical PET Imaging Systems S.A, Oeiras, Portugal

ClearPEM: performance

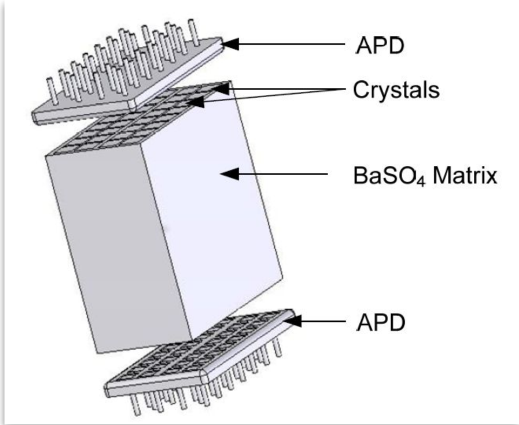

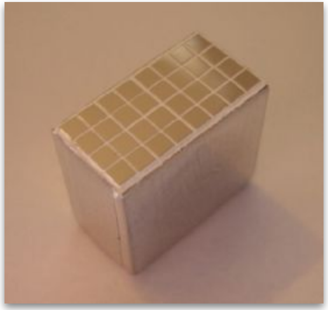

Parameter	Value
Spatial resolution FWHM	1.4 mm
Energy Resolution FWHM	15.5%
CTR res. FWHM	2.8 ns
DOI res. FWHM	3 mm

Prototype installed in **Hopital Nord Marseille** (France), then moved in 2013 to **San Gerardo Hospital in Monza** (Italy)

ClearPEM: clinical images

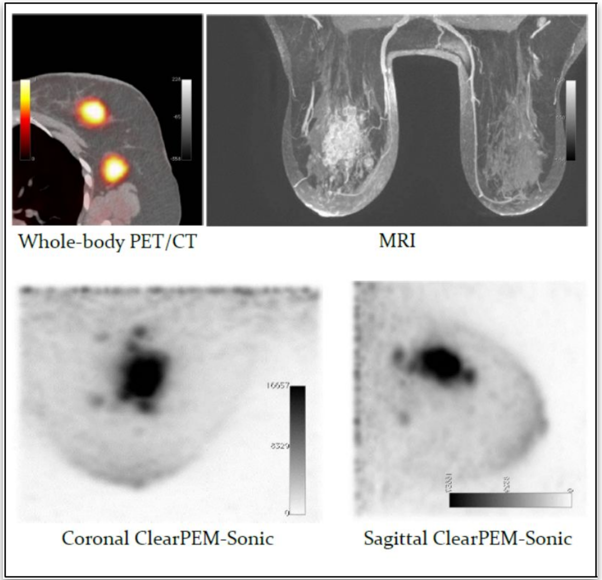

Ability to resolve multifocal lesions

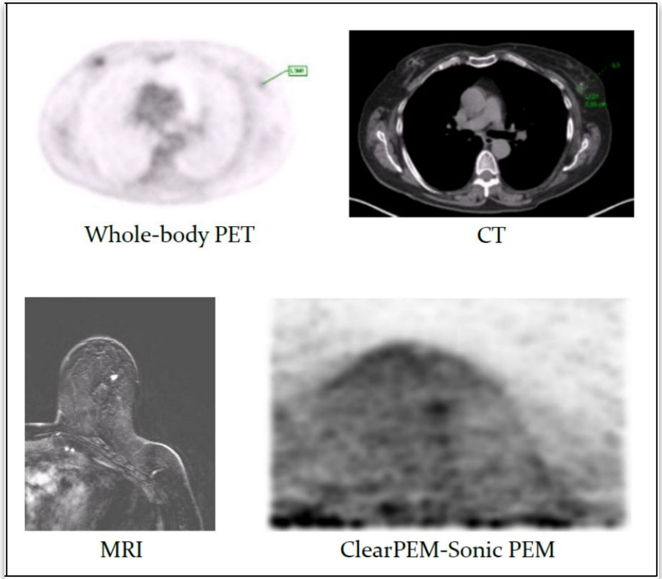

Detection of lesions invisible to WB-PET and CT

EndoTOFPET-US (2011-2018)

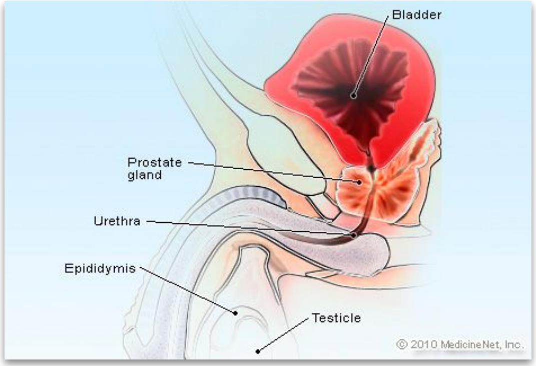

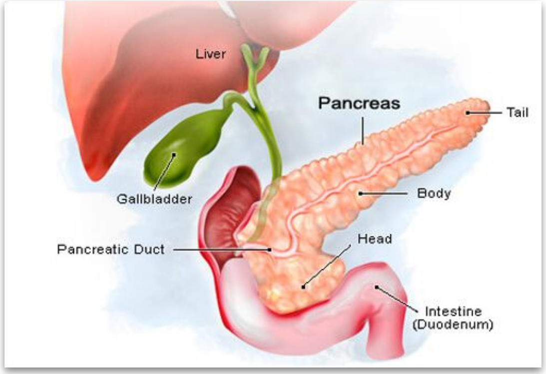

➔ **Target:** prostate and pancreas cancer

- Prostate cancer very common in men
- Pancreatic cancer very aggressive, difficult diagnosis

➔ **Issues:** currently PET/CT do not provide early diagnosis

- Small lesions, below detectability until advanced stage
- Strong background from neighbouring organs (heart, liver, bladder)
- Lack of specific radio-molecules

➔ **Goal:** achieve high spatial resolution and reject background

- Endoscopic approach
- Time of flight around **200 ps FWHM** -> 3 cm

EndoTOFPET-US (2011-2018)

UNIVERSITÀ DEGLI STUDI DI MILANO BICOCCA

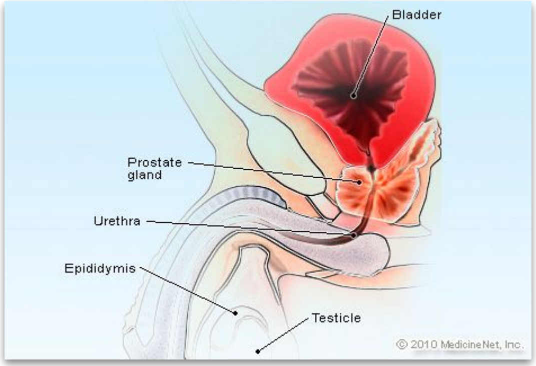

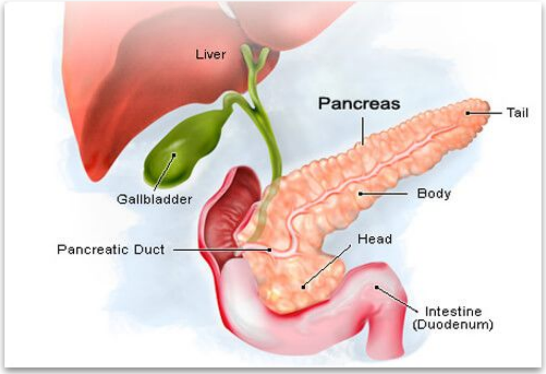

➔ International collaboration in the frame of the **European FP7 program:**

- ➢ 7 academic partners: CERN, DESY, LIP, TU-Delft, TUM, Heidelberg Uni, Milano-Bicocca Uni
- ➢ 3 industrial partners: KLOE, Fibercryst, Surgiceye
- ➢ 3 clinical partners: Aix-Marseille Uni, Klinikum Recht der Isar -TU Munich, Lausanne Uni

EndoTOFPET-US

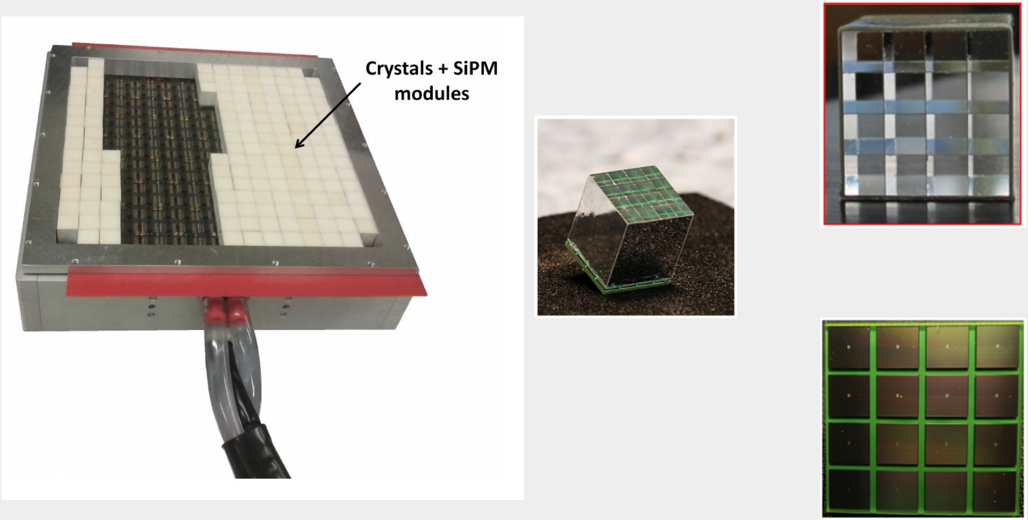

External detector plate

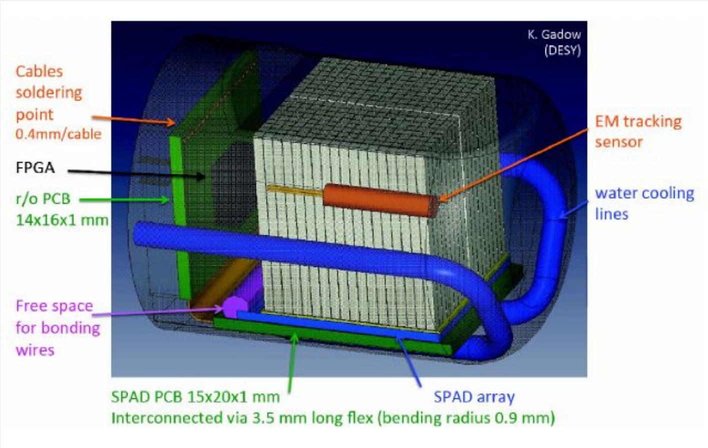

Endoscopic probe

EndoTOFPET-US: timing performance

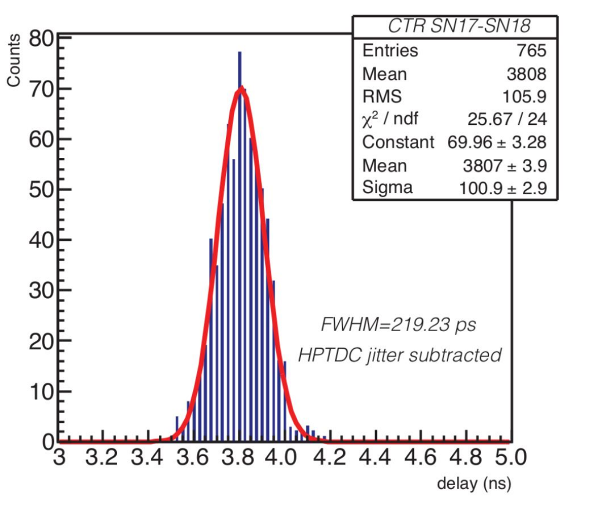

M. Pizzichemi, doi:10.1109/NSSMIC.**2013**.6829146

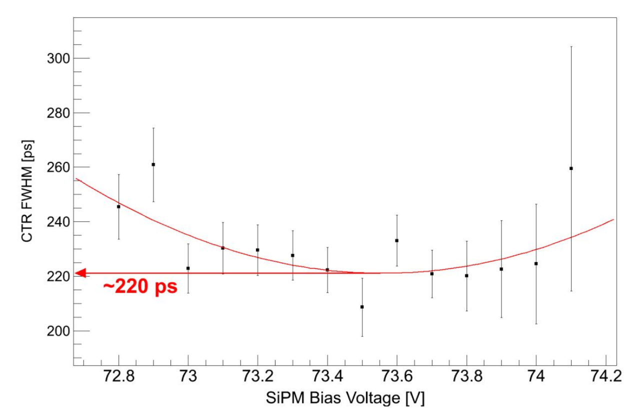

M. Zvolsky J. Phys.: Conf. Ser. 587 012068 - **2015**

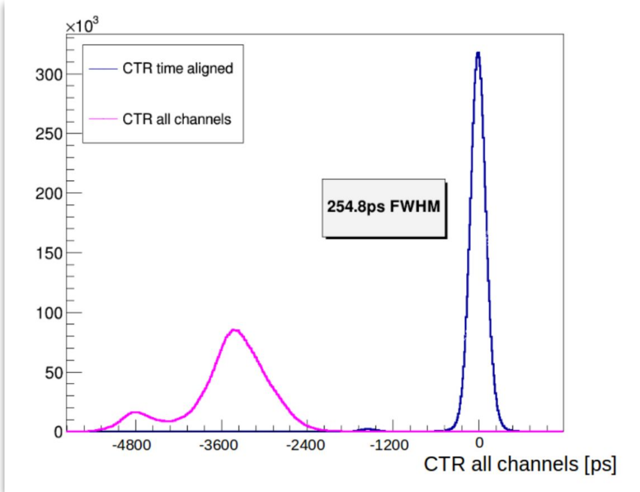

O. Brandt, IEEE NSS/MIC **2018**

- ➔ System timing resolution close to initial goal
- ➔ Several innovative R&Ds (photo-detectors, electronics, light extraction…)
- ➔ Important know-how for future fast timing research

Current PET activities @ Bicocca

State-of-the-art TOF-PET

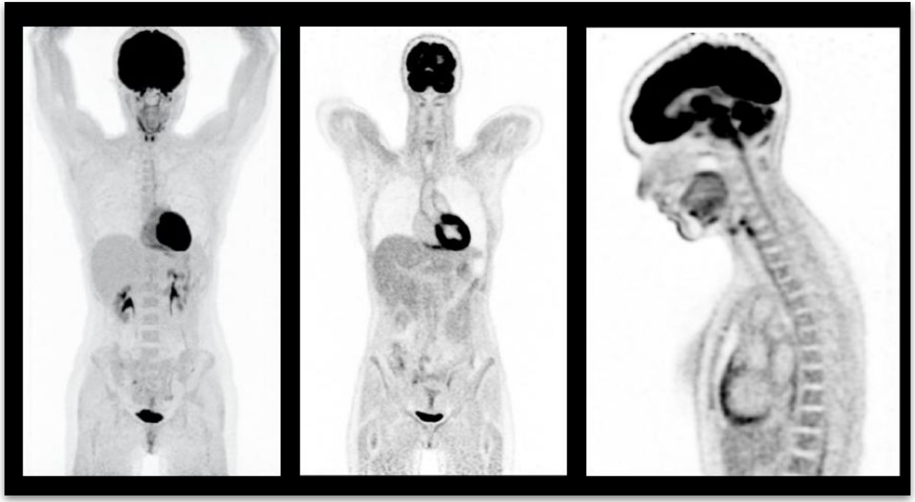

Siemens Biograph Vision (2019) - **205 FWHM** coincidence timing resolution (CTR)

TOF-PET: why more?

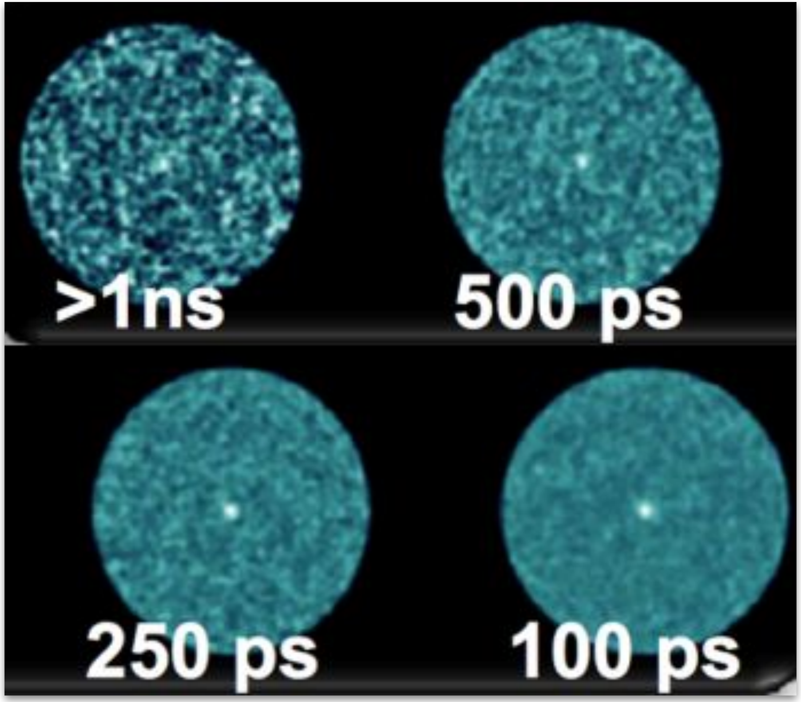

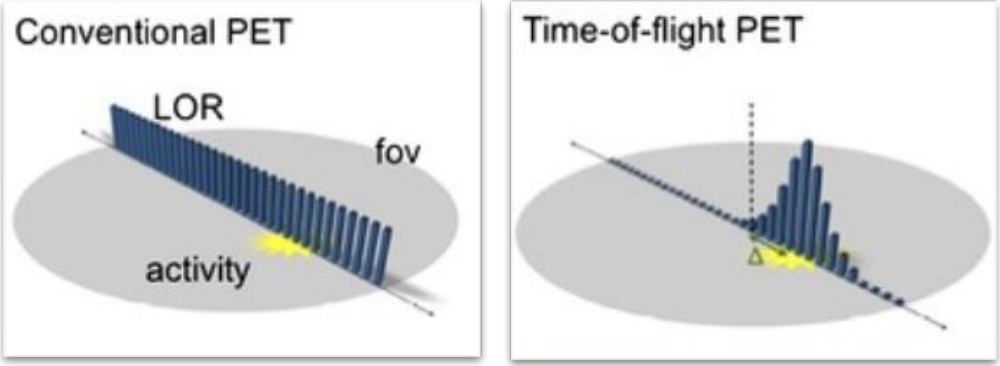

@ 100 ps FWHM CTR

SNR improved by factor 5
effective sensitivity by factor 25

@ 10 ps FWHM CTR

Direct 3D information
Almost reconstruction-less PET

The 10 ps challenge

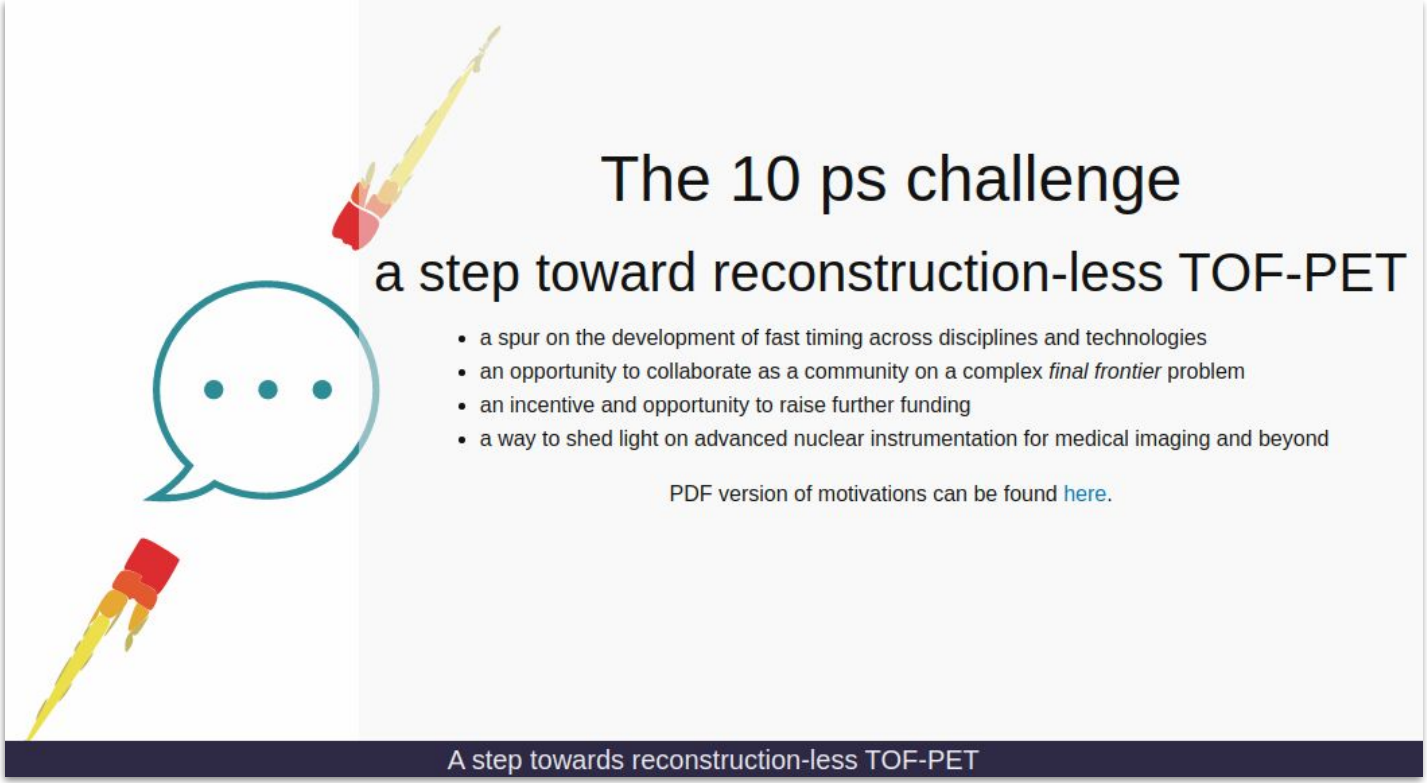

https://the10ps-challenge.org/

Pushing timing towards 10 ps

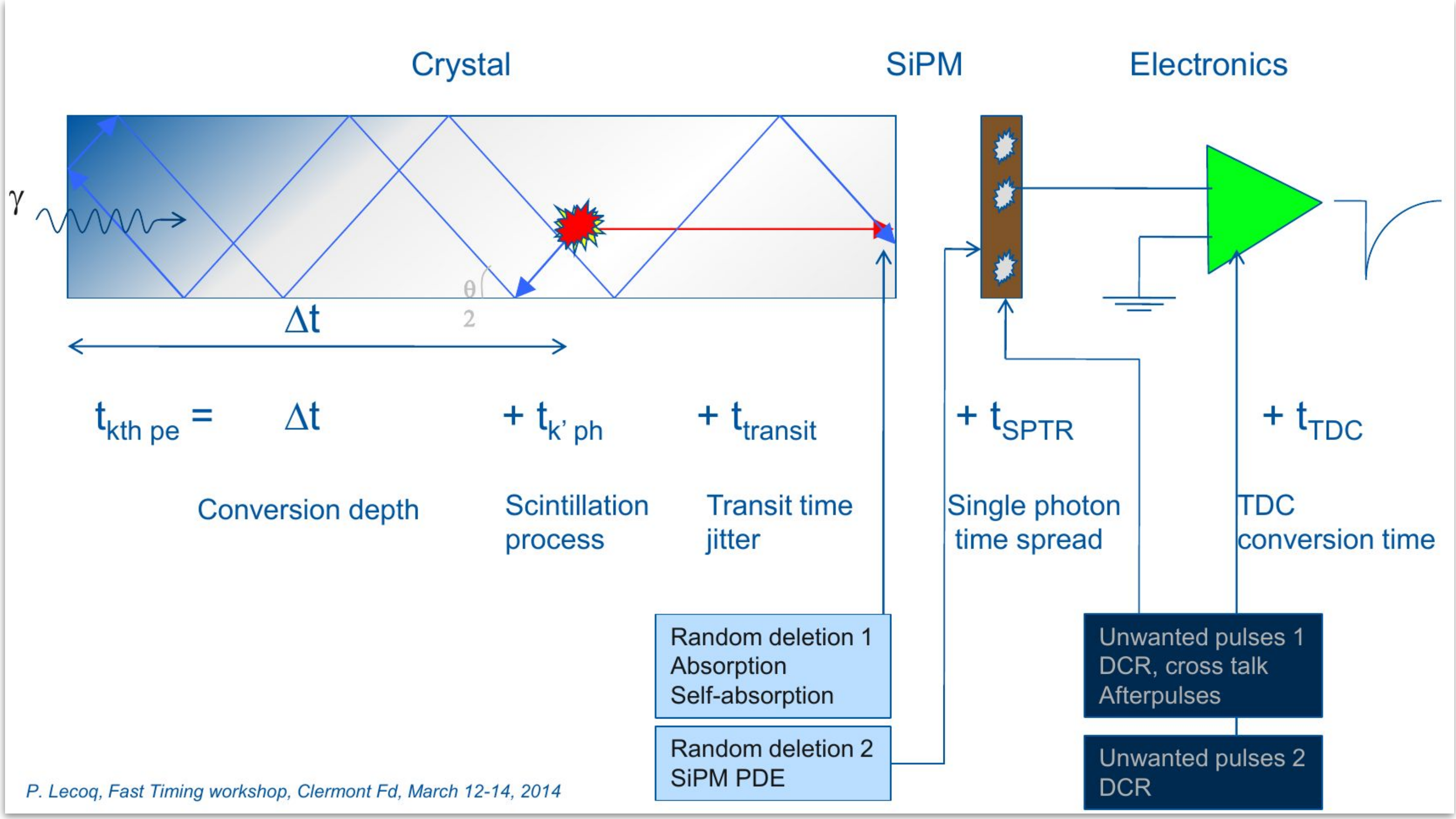

Pushing timing towards 10 ps

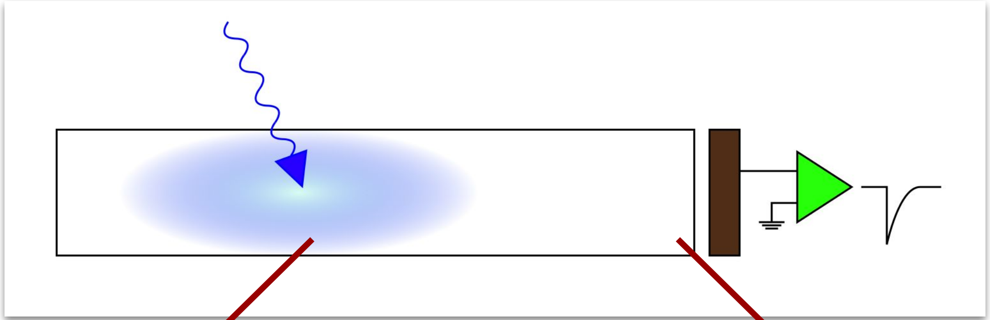

Faster light production

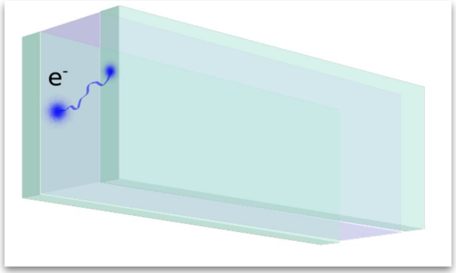

Measurement of DOI

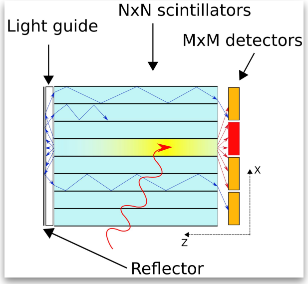

DOI-induced bias of DOI

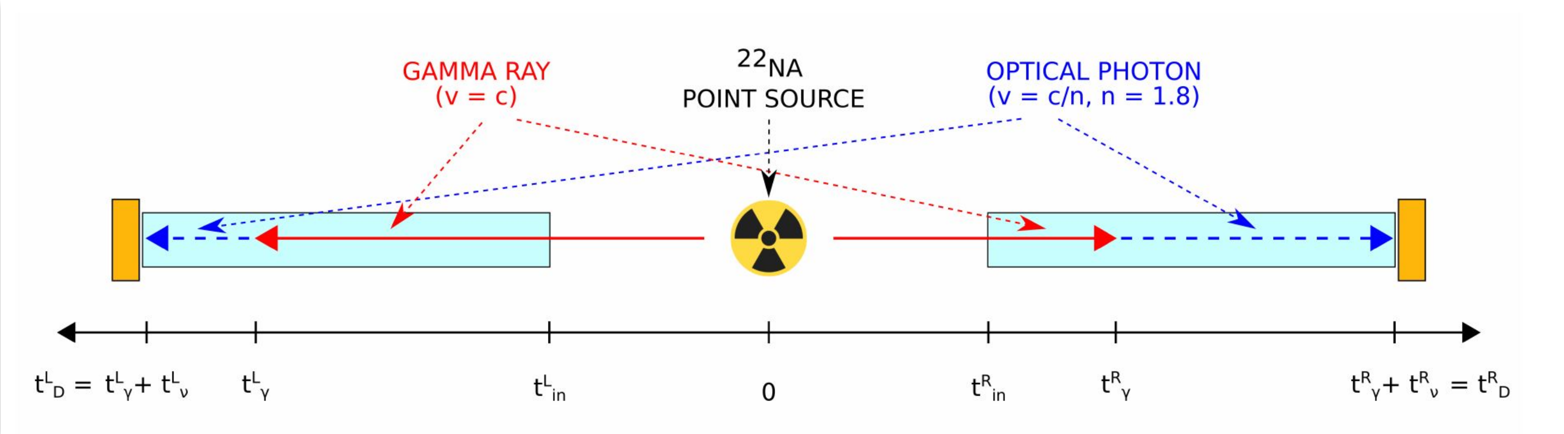

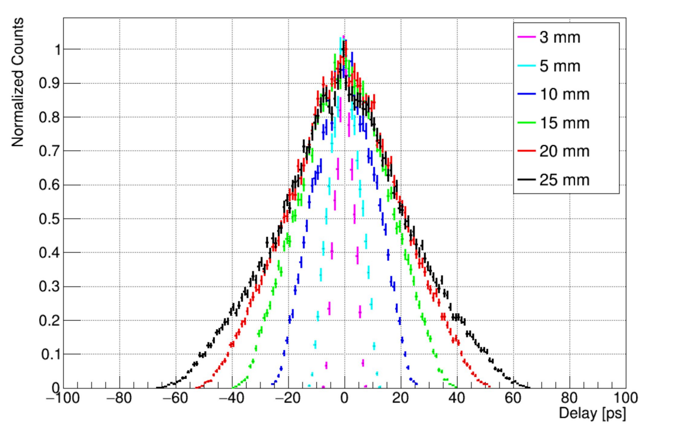

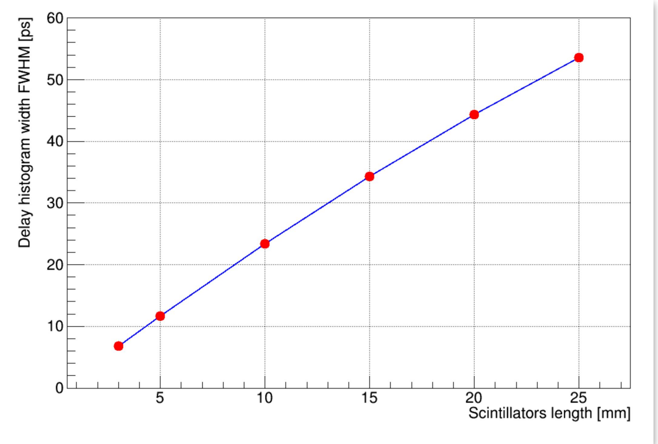

Development of novel DOI module

M. Pizzichemi et al, Phys. Med. Biol. 61 (2016) 4679

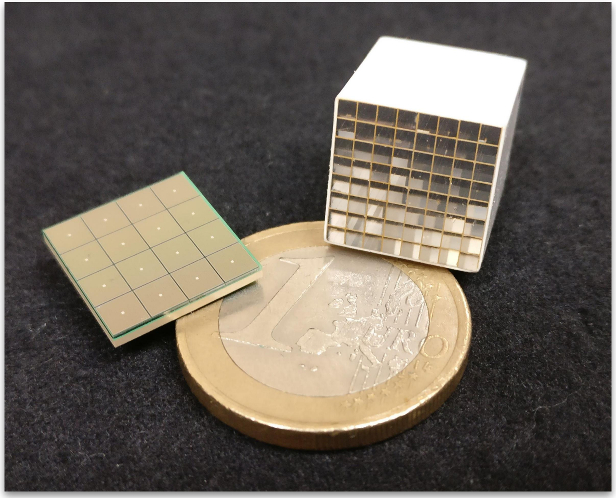

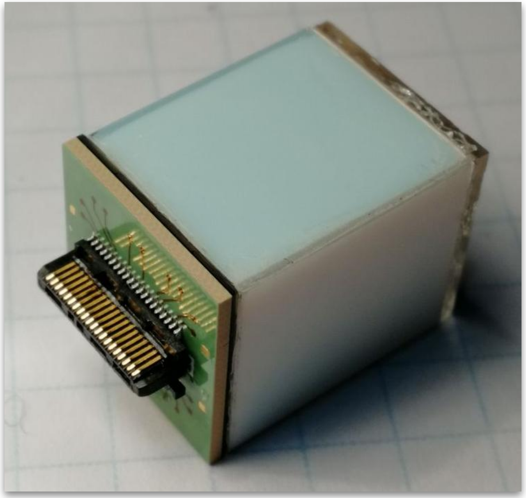

- ➔ Hamamatsu MPPC S13361-3050-AE-04
- ➔ 4x4 channels, each 3x3 mm^2 active area
- ➔ Pulse integration by CAEN DT5740

- ➔ LYSO:Ce array, 8x8 crystals (CPI inc.)
- ➔ ESR reflector by 3M
- ➔ Individual crystal 1.5 x 1.5 x 15 mm^3

Depth of Interaction module

M. Pizzichemi et al, Phys. Med. Biol. 61 (2016) 4679

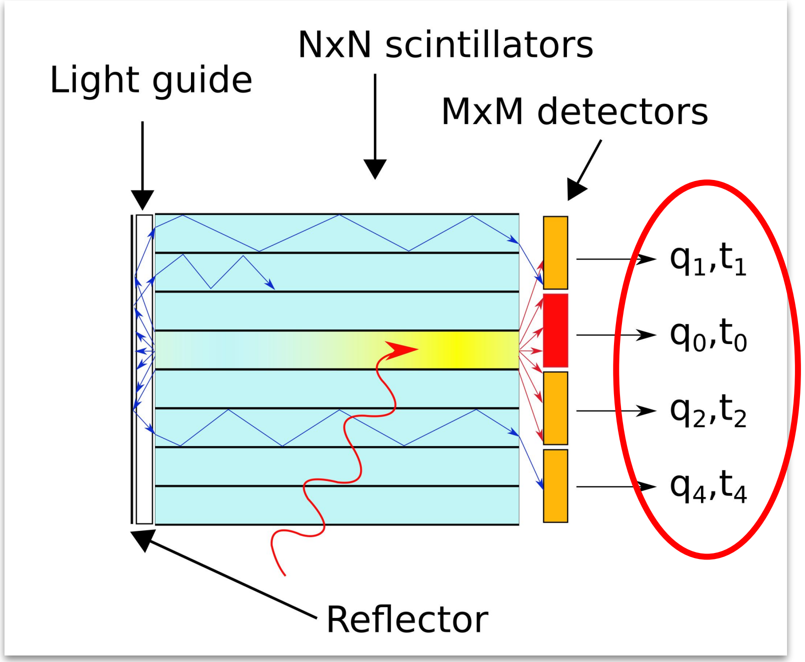

$$Q = \sum_i q_i$$ → **Energy**

$$w = \frac{q_0}{\sum_i q_i}$$ → **DOI**

$$\hat{t}_0 = \frac{\sum_i a_i (t_i - \Delta_i(w))}{\sum_i a_i}$$ → **Timing**

Information distributed on array of detectors, then recombined

Using DOI to improve CTR

M. Pizzichemi et al, Phys. Med. Biol. 64 (2019) 155008

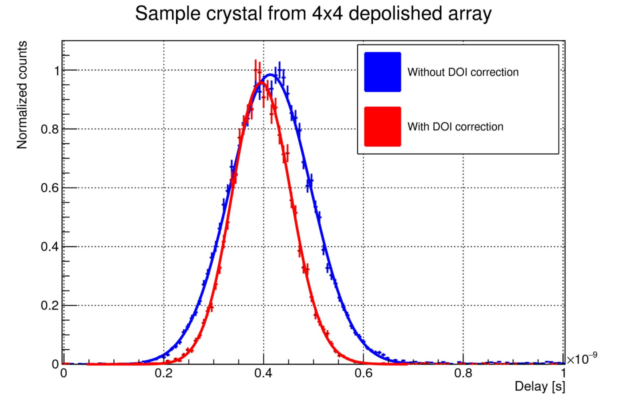

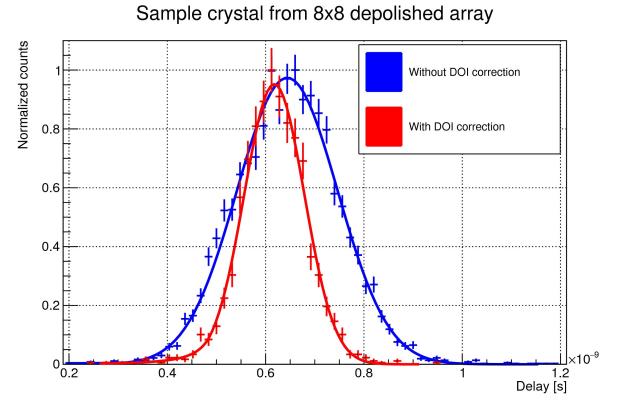

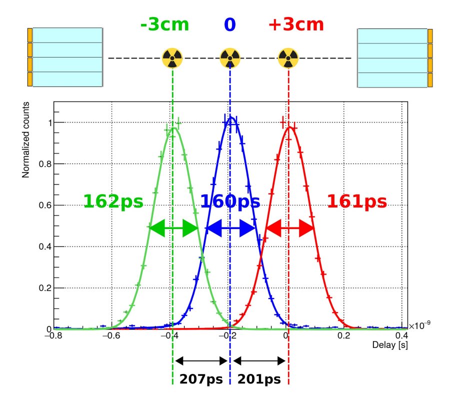

LYSO array type	Crystals dim. [mm^3]	En. Res. FWHM @ 511 keV [%]	DOI Res. FWHM [mm]	CTR FWHM [ps]
4x4	3.1 x 3.1 x 15	9.5 ± 0.2	3.0 ± 0.2	**159 ± 2**
8x8	1.5 x 1.5 x 15	9.9 ± 0.2	3.0 ± 0.2	**157 ± 2**

About **160 ps FWHM CTR** in multiple (64) channel system

Improving DOI with Neural Networks

A. Zetcepin, M. Pizzichemi et al, Phys. Med. Biol. 65 (2020) 175017

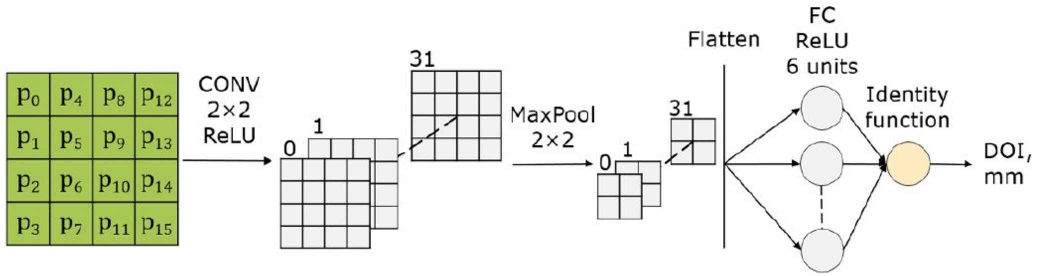

Figure 4. The architecture of the CNN. The network receives 16 integrated charge values arranged in a 4× 4 matrix as an input (in green). The ReLU is employed as an activation function on the convolutional (CONV) and the FC layer. The output layer (in yellow) uses the identity function.

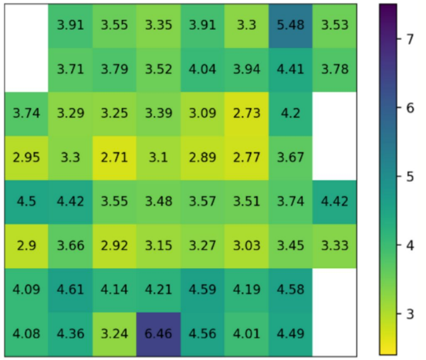

(a) Original method, μ=3.76 mm

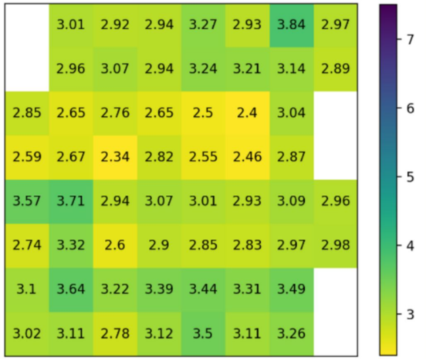

(d) CNN, μ=3.01 mm

- ➔ **Machine learning** approaches investigated to improve the average DOI resolution of LYSO crystal arrays based on light sharing
- ➔ Different **architectures** tested (CNN and DNN)
- ➔ Significant improvement in DOI resolution, especially for **edge crystals**
- ➔ Expected beneficial impact on **image quality**, especially for pre-clinical and organ dedicated PET scanners

Recovery of inter-crystal scatter

A. Polesel PhD Thesis, Università di Milano Bicocca - 2021

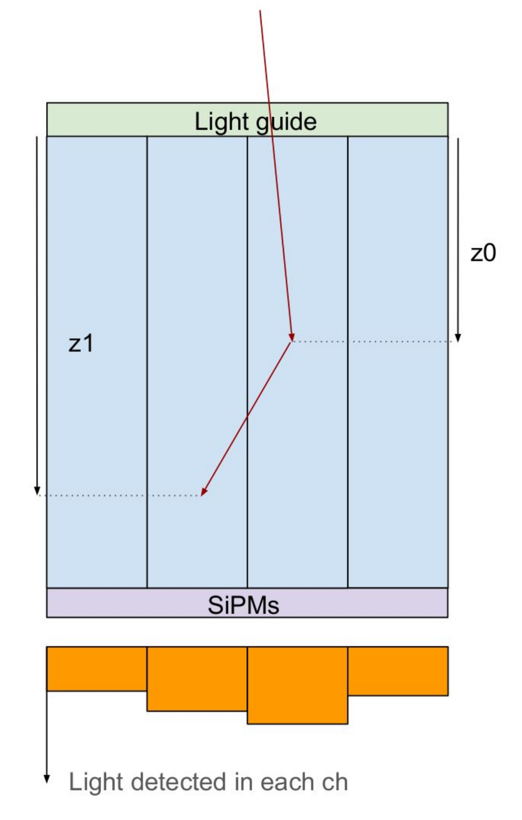

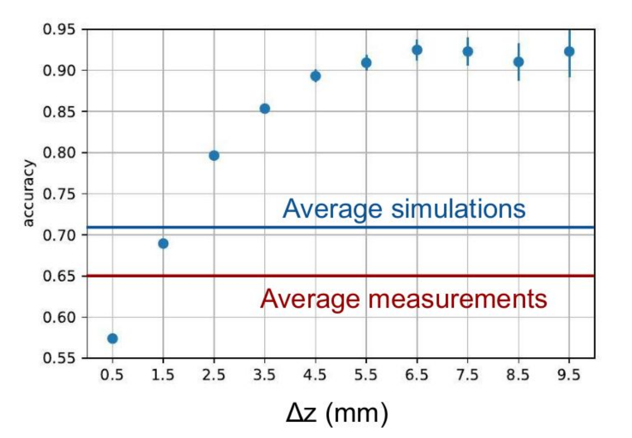

- ➔ Developed algorithm to correctly assign crystal of first interaction in inter-crystal scatter events
- ➔ Positive impact on PET image quality (higher sensitivity with better spatial resolution)
- ➔ Possible applications beyond pure PET (Compton camera)

Array type	Simulations	Measurements	Measurement (50% cut)
4 × 4	(71 ± 1) %	(65.2 ± 0.6) %	(74 ± 1) %
8 × 8	(74 ± 1) %	(68.6 ± 0.5) %	(75 ± 1) %

Heterostructure concept

R. M. Turtos et al, Phys. Med. Biol. 64 (2019) 185018

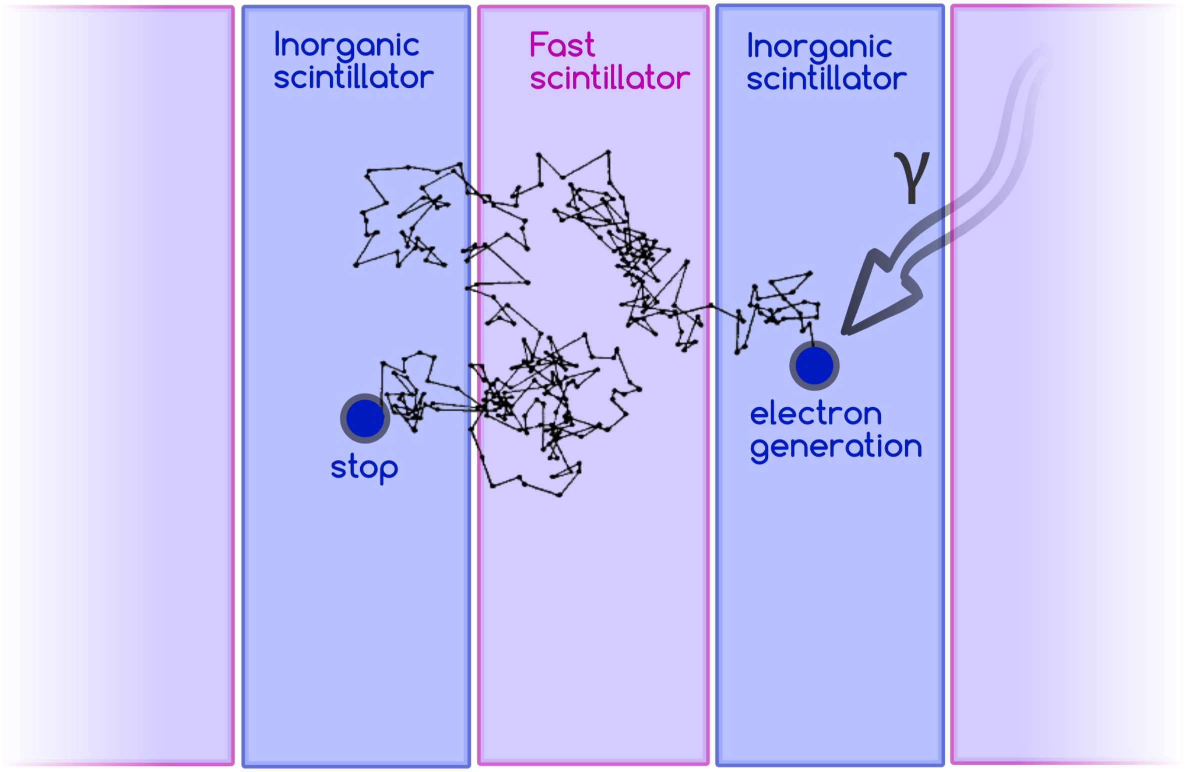

Energy sharing between inorganic and fast scintillator

Heterostructure proof of concept

R. M. Turtos et al, Phys. Med. Biol. 64 (2019) 185018

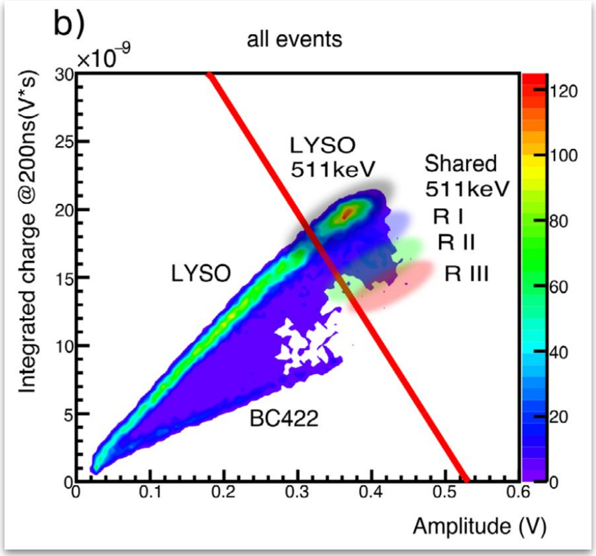

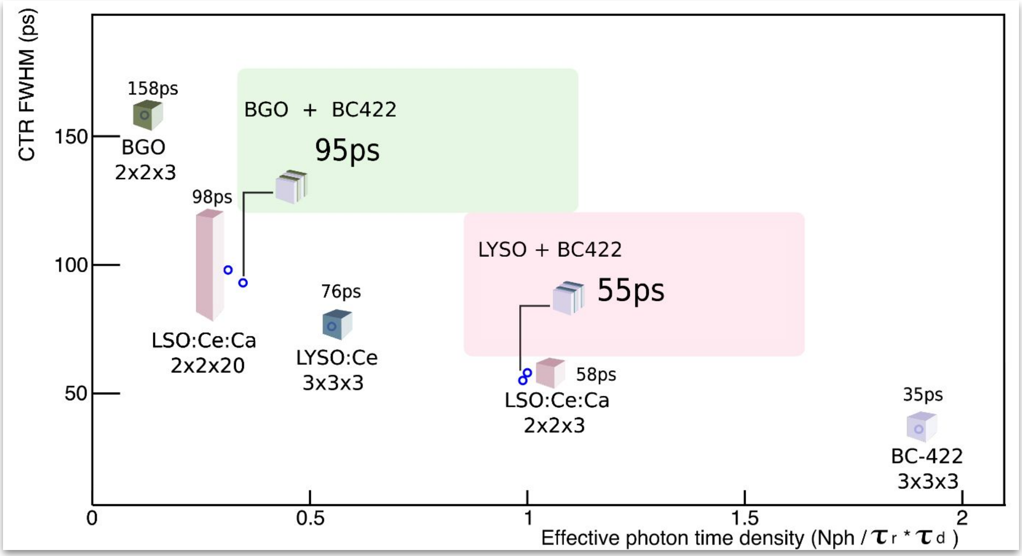

- ➔ Sharing of recoil electron energy between materials demonstrated
- ➔ Timing resolution improved for a fraction of events
  - ➢ BGO+BC-422 -> 95ps FWHM CTR
  - ➢ LYSO+BC-422 -> 55ps FWHM CTR
- ➔ Tests with short pixels, longer pixels will be affected by DOI-induced bias in CTR

Cherenkov and BGO

N. Efthimiou, M. Pizzichemi et al., TRPMS 2020, doi: 10.1109/TRPMS.2020.3048642

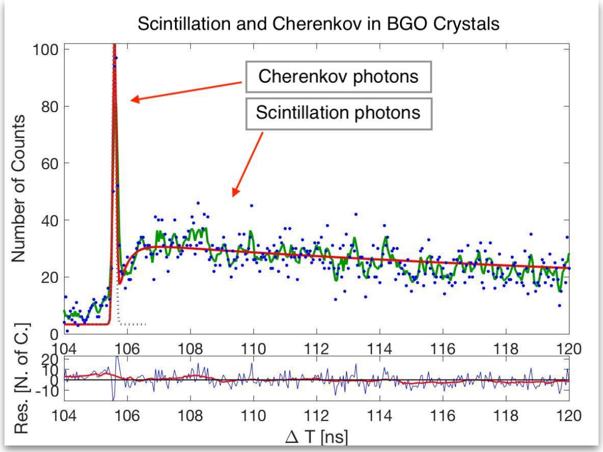

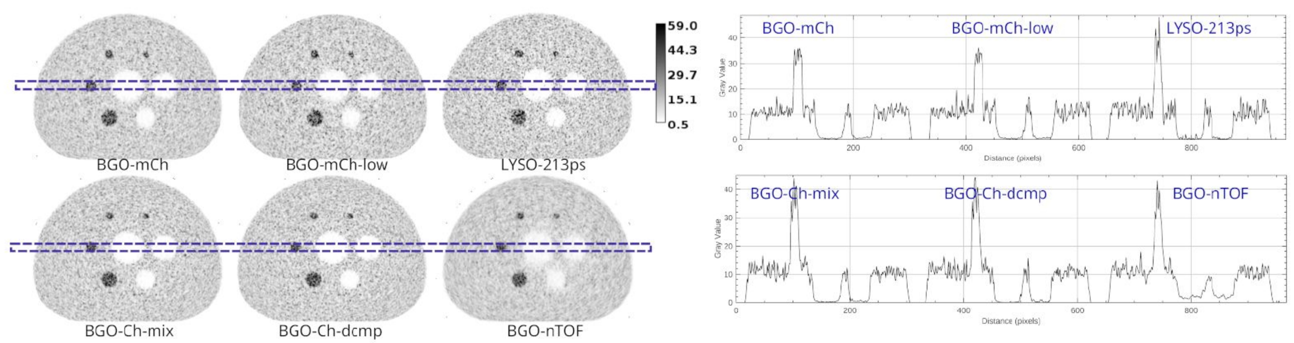

Fig. 7. Reconstructed images at the 40^{th} iteration for the different detector models for one of the noise realisations.

- ➔ Cherenkov radiation used **boost timing capability** of dense, slow scintillators (BGO)
- ➔ Optimization of **ultra-fast detection techniques** in the NUV region
- ➔ Development of **multiple timing kernel reconstruction** algorithms to fully exploit timing information
- ➔ From Monte Carlo simulations, PET scanners based on **BGO** with Cherenkov can provide **similar image quality** to best available TOF-PET scanners (Siemens Biograph Vision, TOF 205 ps), with **better Contrast-to-Noise ratio** due to higher sensitivity

Cherenkov in semiconductors

G. Terragni Master Thesis, Università di Milano Bicocca - 2021

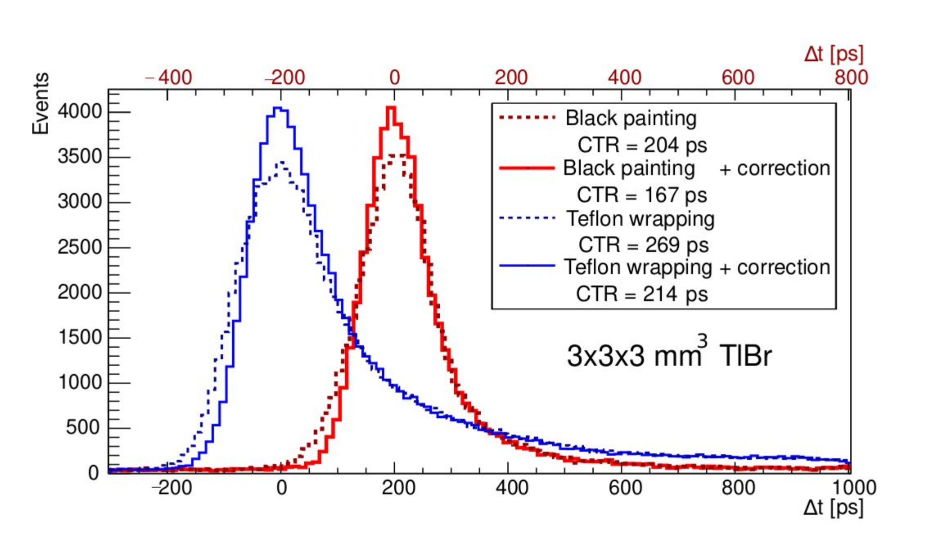

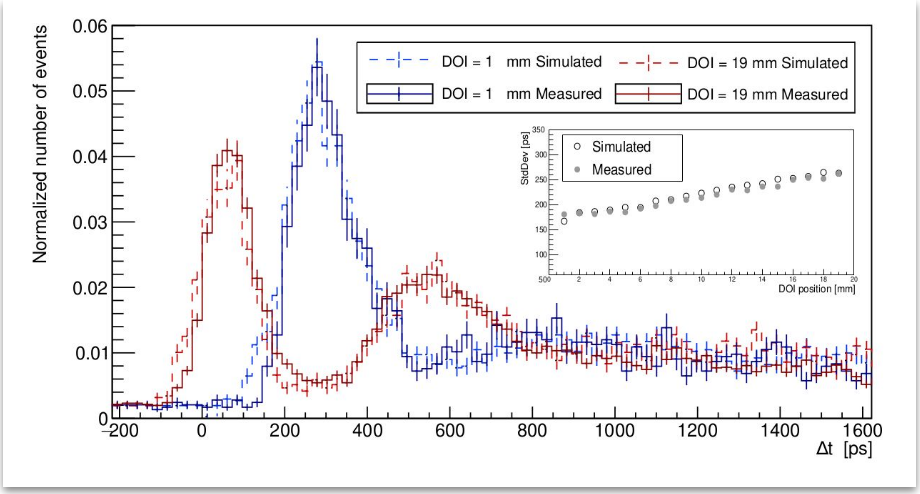

- ➔ Semiconductor gamma ray detectors (e.g. TlBr) show **extremely good energy resolution** (about 2-3% FWHM), but poor timing resolution
- ➔ Combining with detection of **Cherenkov photons** can lead to outstanding overall performance

Heterostructures and DOI

M. Pizzichemi et al, NSS-MIC Conference, Manchester (2019)

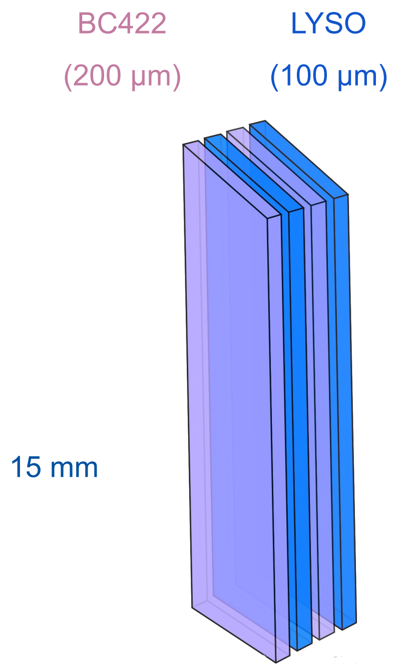

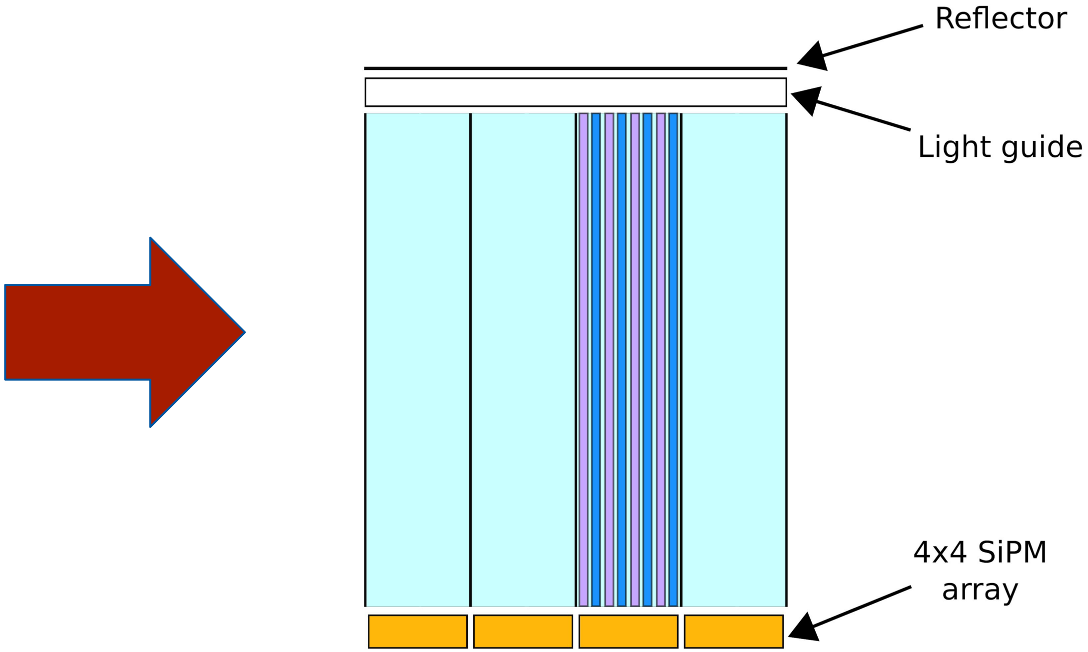

Heterostructures and DOI

M. Pizzichemi et al, NSS-MIC Conference, Manchester (2019)

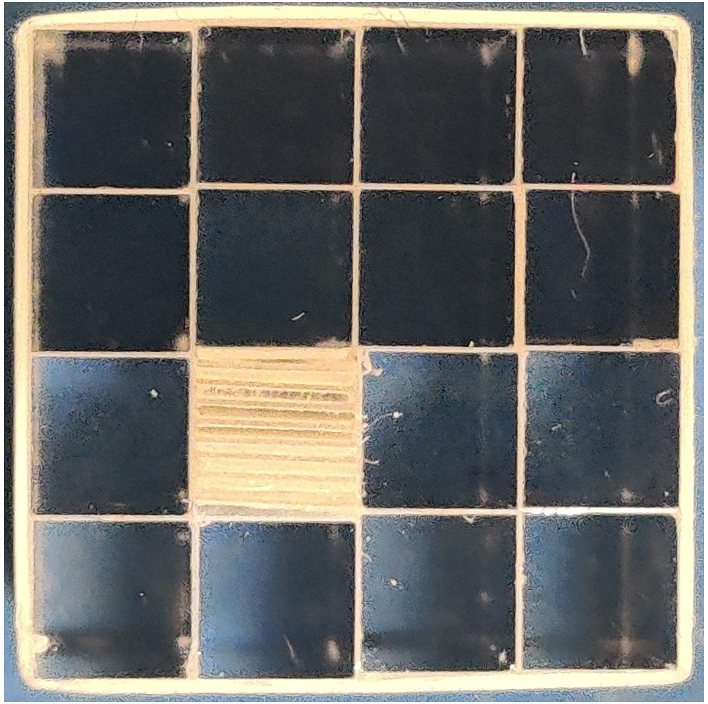

Heterostructures and DOI

M. Pizzichemi et al, NSS-MIC Conference, Manchester (2019)

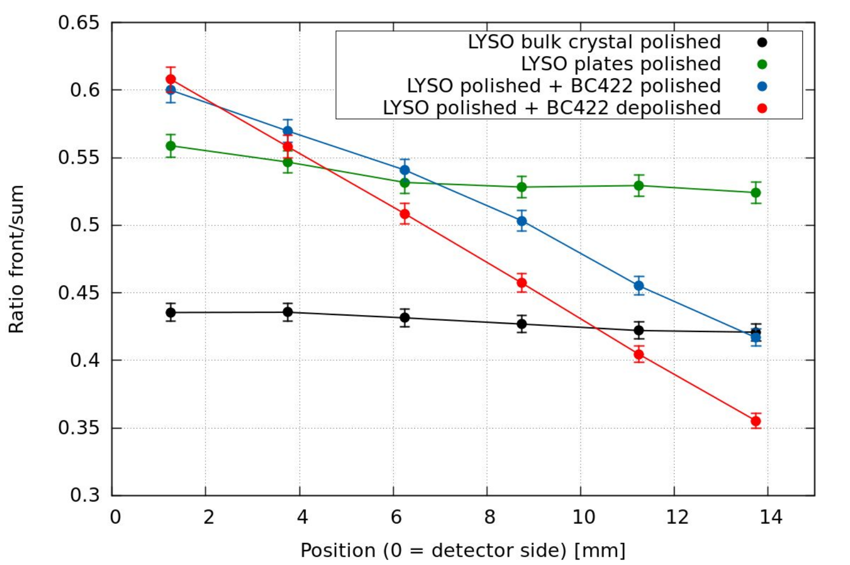

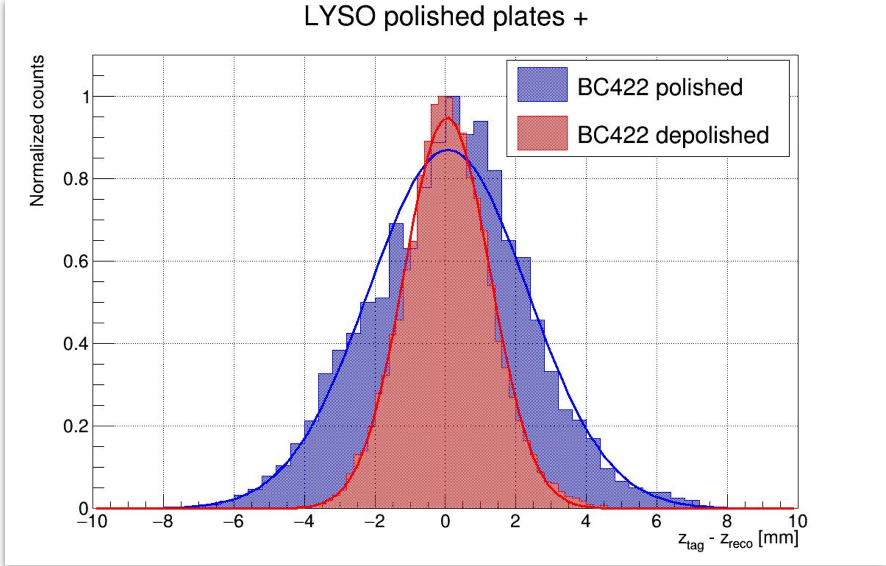

	LYSO poli + BC422 poli	LYSO poli + BC422 depo
DOI (FWHM)	**4.9 ± 0.1 mm**	**2.2 ± 0.1 mm**

Radiation Hard Scintillating Materials

L. Martinazzoli, et al. NIM A 2021, https://doi.org/10.1016/j.nima.2021.165231

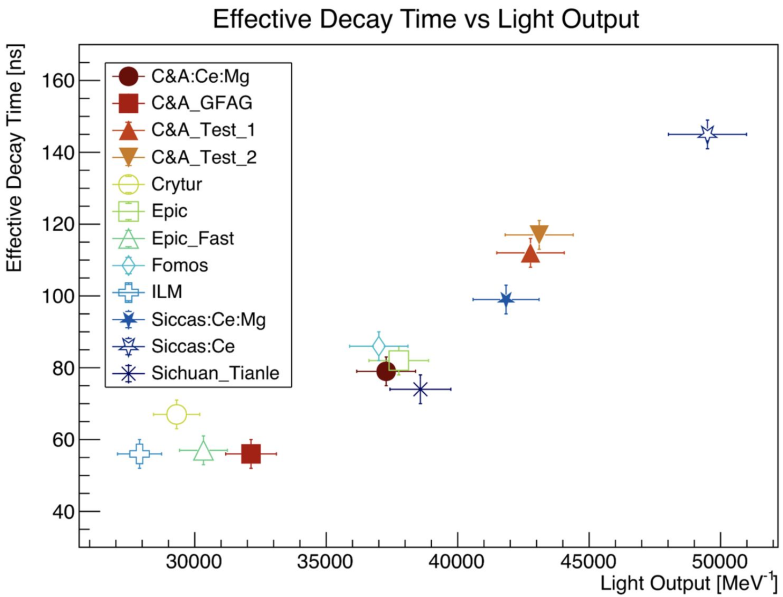

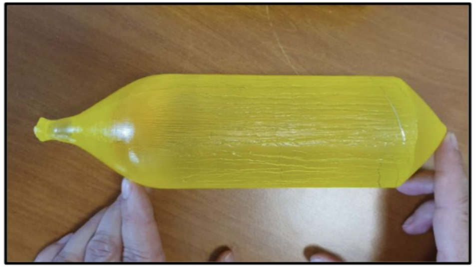

GAGG ingot, courtesy of K. Lebbou, Institute Lumière Matière, Lyon

➔ Studies of **radiation-hard scintillating materials** for applications at future colliders

➔ Characterisation and performance evaluation in terms of light output, scintillation kinematics, and time resolution

Scintillating Fibres-based Calorimetry

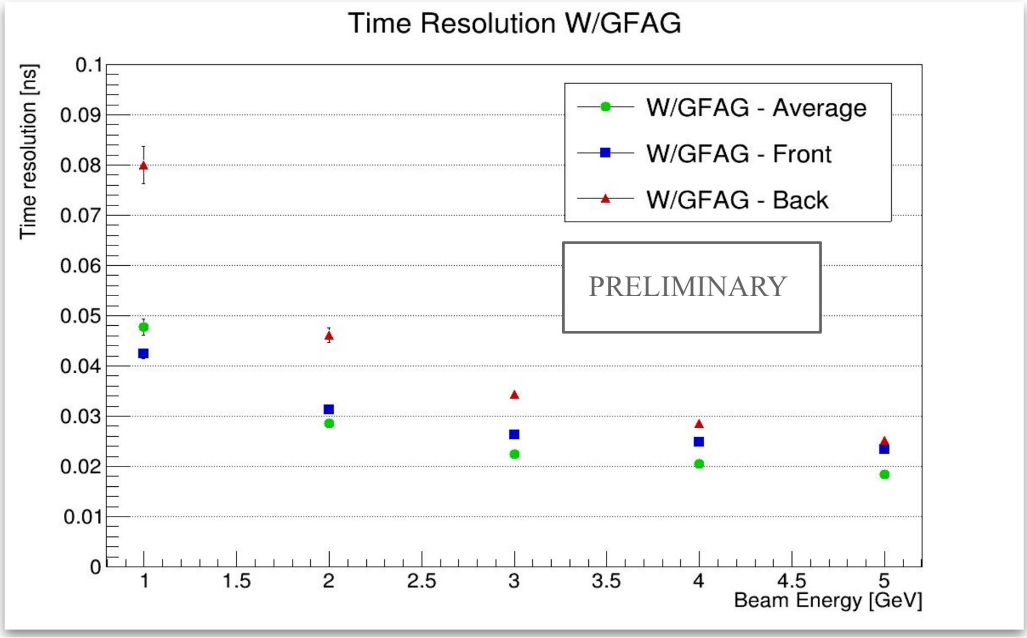

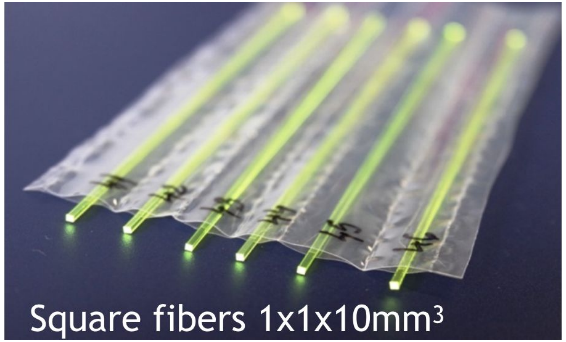

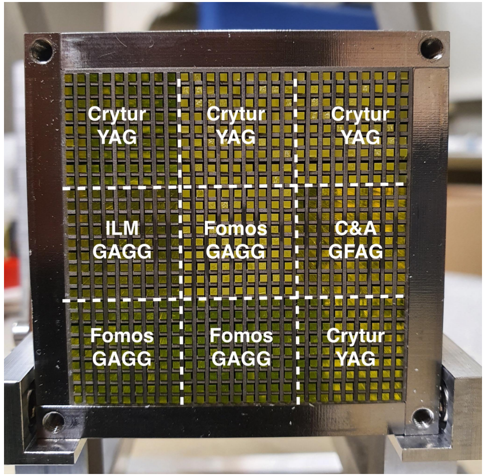

- ➔ Prototyping of **Spaghetti Calorimeters (SPACAL)** with radiation-hard scintillating fibres
- ➔ Experimental testing at testbeam facilities: **< 20 ps @ 5 GeV**
- ➔ Study and development of novel techniques for time measurement with **picosecond resolution**

Conclusions

- ➔ Unimib group active in PET research since more than 10 years
- ➔ Participation to several international collaborations
- ➔ Initial focus on development of organ dedicated PET scanners
- ➔ Current focus on fast timing, with ultimate goal set to 10 ps TOF-PET
- ➔ Several R&D lines, in medical physics as well as HEP

Thank you for your attention!

marco.pizzichemi1@unimib.it